

Article

Stereoselective cyclopropanation of electrondeficient olefins with a cofactor redesigned carbene transferase featuring radical reactivity

Daniela M Carminati, and Rudi Fasan

ACS Catal., Just Accepted Manuscript • DOI: 10.1021/acscatal.9b02272 • Publication Date (Web): 05 Sep 2019

Downloaded from pubs.acs.org on September 9, 2019

Just Accepted

“Just Accepted” manuscripts have been peer-reviewed and accepted for publication. They are posted online prior to technical editing, formatting for publication and author proofing. The American Chemical Society provides “Just Accepted” as a service to the research community to expedite the dissemination of scientific material as soon as possible after acceptance. “Just Accepted” manuscripts appear in full in PDF format accompanied by an HTML abstract. “Just Accepted” manuscripts have been fully peer reviewed, but should not be considered the official version of record. They are citable by the Digital Object Identifier (DOI®). “Just Accepted” is an optional service offered to authors. Therefore, the “Just Accepted” Web site may not include all articles that will be published in the journal. After a manuscript is technically edited and formatted, it will be removed from the “Just Accepted” Web site and published as an ASAP article. Note that technical editing may introduce minor changes to the manuscript text and/or graphics which could affect content, and all legal disclaimers and ethical guidelines that apply to the journal pertain. ACS cannot be held responsible for errors or consequences arising from the use of information contained in these “Just Accepted” manuscripts.

1
2
3
4
5
6
7
8
9
10
11
12
13
14
15
16
17
18
19
20
21

Stereoselective cyclopropanation of electrondeficient olefins with a cofactor redesigned carbene transferase featuring radical reactivity

22
23
24
25
26
27
28
29
30
31
32
33
34
35
36
37
38
39
40
41
42
43
44
45
46
47
48
49
50
51
52

Daniela M. Carminati^a and Rudi Fasan^{*,a}

^aDepartment of Chemistry, University of Rochester, Rochester, NY 14627, United States.

ABSTRACT: Engineered myoglobins and other hemoproteins have recently emerged as promising catalysts for asymmetric olefin cyclopropanation reactions via carbene transfer chemistry. Despite this progress, the transformation of electron-poor alkenes has proven very challenging using these systems. Here, we describe the design of a myoglobin-based carbene transferase incorporating a non-native iron-porphyrin cofactor and axial ligand, as an efficient catalyst for the asymmetric cyclopropanation of electron-deficient alkenes. Using this metalloenzyme, a broad range of both electron-rich and electron-deficient alkenes are cyclopropanated with high efficiency and high diastereo- and enantioselectivity (up to >99% *de* and *ee*). Mechanistic studies revealed that the expanded reaction scope of this carbene transferase is dependent upon the acquisition of metallocarbene radical reactivity as a result of the reconfigured coordination environment around the metal center. The radical-based reactivity of this system diverges from the electrophilic reactivity of myoglobin and most of known organometallic carbene transfer catalysts. This work showcases the value of cofactor redesign toward tuning and expanding the reactivity of metalloproteins in abiological reactions and it provides a biocatalytic solution to the asymmetric cyclopropanation of electrodeficient alkenes. The metallocarbene radical reactivity exhibited by this biocatalyst is anticipated to prove useful in the context of a variety of other synthetic transformations.

53
54
55
56
57
58
59
60

KEYWORDS: Cyclopropanation, electrondeficient olefins, myoglobin, carbene transfer catalysis, radical mechanism, Hammett

Introduction

The metal-catalyzed cyclopropanation of alkenes with diazo compounds constitutes a convenient and direct strategy for the construction of cyclopropane rings,¹⁻⁴ which are key structural motifs found in many drug molecules and biologically active natural products.⁵⁻⁸ While several transition metal complexes have proven effective for executing olefin cyclopropanations via carbene transfer chemistry,¹⁻⁴ the development of biocatalytic strategies for realizing these transformations is highly desirable toward the implementation of sustainable methods for chemical synthesis. Over the past few years, iron-based heme-containing proteins and enzymes, such as myoglobins⁹⁻¹³ and cytochrome P450s¹⁴⁻¹⁸, respectively, have been identified as promising biocatalysts for promoting olefin cyclopropanation reactions with diazo compounds. In particular, our group previously reported the ability of engineered variants of sperm whale myoglobin (Mb) to catalyze the asymmetric cyclopropanation of vinylstyrenes in the presence of ethyl α -diazoacetate (EDA)^{9, 10} or other acceptor-only diazo compounds,^{11, 12} with high levels of diastereo- and enantioselectivity. Artificial metalloenzymes have also been developed and investigated for promoting abiological cyclopropanation reactions.¹⁹⁻²⁵

Recent experimental and computational studies have provided insights into the mechanism of hemoprotein-catalyzed cyclopropanation reactions^{9, 26-28} and the role of the protein scaffold in controlling the stereoselectivity of these transformations.²⁹ These studies support a mechanistic scenario in which an heme-carbenoid intermediate is initially formed upon reaction of the ferrous hemoprotein with the diazo reagent. This intermediate was shown to possess electrophilic reactivity^{9, 26} and be capable of engaging olefins and other nucleophiles³⁰⁻³² in a carbene transfer reaction manifold. In the context of iron-porphyrin and hemoprotein-catalyzed intermolecular cyclopropanations with α -diazo esters, computational and experimental analyses support a catalytic mechanism involving a concerted, asynchronous insertion of the heme-bound carbene into the C=C bond of the olefin substrate.^{27, 29}

Despite the progress made in developing biocatalytic strategies for olefin cyclopropanation, the scope of these transformations has been largely restricted so far to aryl-substituted and aliphatic olefins, limiting the types of cyclopropane structures accessible using biocatalysis. In particular, the cyclopropanation of electron-deficient olefins has remained a largely unmet goal in this area.

1
2
3 In the presence of diazoesters, these transformations can give access to electrophilic cyclopropanes
4 carrying two electron-withdrawing groups, which represent valuable building blocks for medicinal
5 chemistry as well as key intermediates for various synthetic applications.³³⁻³⁵ While currently
6 lacking, biocatalytic approaches for realizing these transformations would be highly desirable.
7
8

9
10 Modification of the metal coordination environment can have a profound effect on the
11 functional properties in metalloenzymes/proteins.^{18, 20, 21, 24, 36-48} In previous work, we
12 demonstrated how alteration of the heme cofactor environment in myoglobin through substitution
13 of the metal center,^{20, 49, 50} ‘proximal’ residue,^{20, 42} and/or porphyrin ligand,²¹ can alter the reactivity
14 of this metalloprotein in the context of non-native nitrene and carbene transfer reactions. Here, we
15 report the design of a cofactor-reconfigured myoglobin-based catalyst useful for the stereoselective
16 cyclopropanation of electron-deficient olefins with diazoesters. Mechanistic studies show how the
17 expanded reaction scope of this metalloprotein toward these challenging substrates is dependent
18 upon the acquisition of radical carbene transfer reactivity and a dramatic change in the
19 cyclopropanation mechanism, as a result of the combined effect of the non-native iron-porphyrin
20 cofactor and axial ligand integrated into this metalloprotein.
21
22
23
24
25
26
27
28
29

30 31 **Results and Discussion**

32 33 **Design and Generation of Cofactor Reconfigured Carbene Transferase**

34
35 The reactivity of myoglobin (Mb) in carbene transfer reactions stems from its heme cofactor
36 (iron-protoporphyrin IX), which is coordinated at the iron center by the side-chain imidazolyl
37 group of a conserved histidine residue (His93 in sperm whale myoglobin) as the ‘proximal’ axial
38 ligand.⁵¹ The latter contributes to anchor the cofactor to the protein and participate in modulating
39 both the redox and the oxygen binding properties of this metalloprotein.⁵¹ While engineered Mb
40 have proven to be effective catalysts for the cyclopropanation of aryl-substituted olefins and
41 aliphatic olefins,^{9, 10, 12, 29} the cyclopropanation of electron-deficient olefins has proven challenging
42 using these systems. Notably, the cyclopropanation of electron-deficient alkenes has represented
43 a notorious challenge also for synthetic carbene transfer catalysts,⁵²⁻⁵⁴ a phenomenon attributed to
44 the electrophilic character of the metal-bound carbenes typically involved in these reactions.
45
46
47
48
49
50
51

52 To overcome these limitations, we envisioned the possibility of enhancing the electrophilic
53 reactivity of the heme-carbene intermediate through modification of the heme cofactor and
54
55
56
57
58
59
60

1
2
3 proximal ligand, as these are bound to directly influence the electronic properties of this reactive
4 species in Mb-mediated cyclopropanation.²⁷ As the parent scaffold for harboring these
5 substitutions, we selected our previously reported variant Mb(H64V,V68A) (**1**, **Figure 1a**) due to
6 its excellent stereoselectivity (>90-99% *de* and *ee*) and broad substrate scope in the
7 cyclopropanation of vinylarenes with EDA.^{9, 10} Based on the considerations outlined above, we
8 decided to substitute the native heme in Mb(H64V,V68A) (**1**) with iron-2,4-diacetyl
9 deuteroporphyrin IX (Fe(DADP)) (**Figure 1a**), an electron-deficient heme analog amenable to
10 incorporation into this hemoprotein.³⁷ The incorporation of Fe(DADP) was previously shown to
11 increase the Fe³⁺/Fe²⁺ reduction potential (E° ; couple) of Mb,³⁷ a result consistent with the effect
12 of the electronwithdrawing acetyl groups conjugated to the tetrapyrrole ring toward destabilizing
13 the ferric form of the metalloprotein. This non-native cofactor was thus expected to potentially
14 enhance the electrophilic character of the heme-carbene intermediate in the context of
15 cyclopropanation reactions. Given the critical role of the proximal axial ligand in affecting the
16 functional properties of myoglobin, we designed a second variant in which the Fe(DADP) cofactor
17 is coordinated at the axial position by the non-canonical amino acid *N*-methyl-histidine (NMH,
18 **Figure 1a**) in place of the native histidine ligand (His 93). This substitution was also reported to
19 increase the E° of Mb,⁴⁶ an effect attributed to the loss of a hydrogen bond interaction between the
20 proximal His ligand and a serine residue within the proximal pocket of the protein.^{55, 56} The
21 aforementioned cofactor and axial ligand modifications were thus envisioned to potentially
22 cooperate toward affecting the reactivity of the Mb-based as a carbene transferase, with the change
23 in redox properties providing a proxy for such additive or synergistic effect.

24
25
26
27
28
29
30
31
32
33
34
35
36
37
38
39
40 The corresponding Mb variants, Mb(H64V,V68A)[Fe(DADP)] (**2**) and
41 Mb(H64V,V68A,H93NMH)[Fe(DADP)] (**3**), could be successfully produced and isolated from *E.*
42 *coli* in good yields (23 and 5 mg protein/L culture, respectively). Incorporation of the non-native
43 Fe(DADP) cofactor was effectively achieved by adapting a protocol previously used for the
44 recombinant production of cofactor-substituted variants of Mb^{20, 21} and other hemoproteins,⁵⁷
45 whereas NHM was introduced at the axial position via amber stop codon suppression⁵⁸ in *E. coli*
46 cells co-expressing an orthogonal aminoacyl-tRNA/tRNA pair specifically evolved for genetic
47 incorporation of this non-canonical amino acid.⁵⁹
48
49
50
51
52
53
54
55
56
57
58
59
60

Characterization of Fe(DADP)-based Mb variants

Characterization of Mb(H64V,V68A)[Fe(DADP)] (2) and Mb(H64V,V68A,H93NMH)[Fe(DADP)] (3) by UV-vis spectroscopy showed a small blue-shift of the Soret band of the Fe(DADP) complex upon incorporation into these proteins (412-415 nm vs. 417 nm for Fe(DADP) alone; **Figure 1b** and **1c**). Incubation of the Mb variants with sodium dithionite induces a shift of the Soret band from 415 nm to 434 and from 412 nm to 430 nm, respectively, corresponding to reduction of the protein from the ferric to the ferrous form. Further incubation with carbon monoxide resulted in a further shift of the Soret band to 434 and 430 nm, respectively, corresponding to CO-bound complex. Overall, the spectral features of the cofactor-substituted variants in their ferric, ferrous, and CO-bound form are similar, albeit not identical, to each other and compared to the heme-containing counterpart (**Figure S1**).

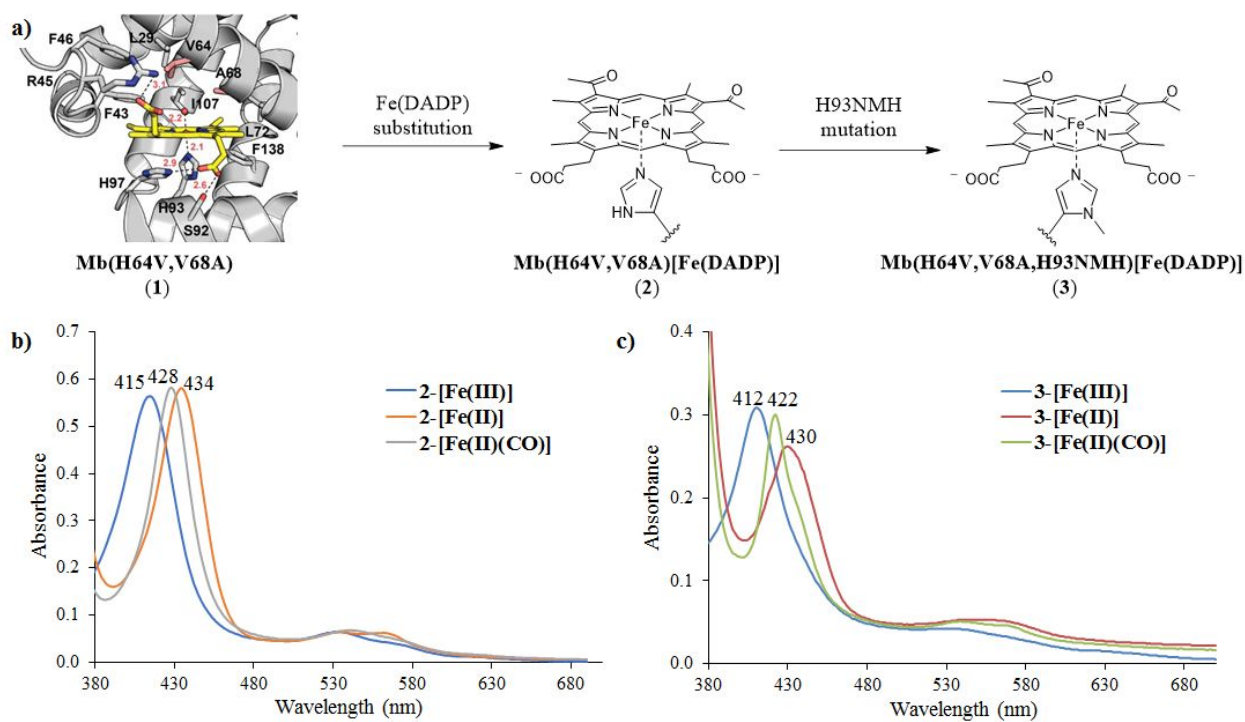


Figure 1. a) High-resolution crystal structure²⁹ of sperm whale Mb(H64V,V68A) (1) and structure of histidine- and N-methyl-histidine-ligated Fe(DADP) cofactor. b) Absorption spectra for ferric, ferrous and CO-bound form of Mb(H64V,V68A)[Fe(DADP)] (2). c) Absorption spectra for ferric, ferrous and CO-bound form of Mb(H64V,V68A,H93NMH)[Fe(DADP)] (3). See **Figure S1** for spectra corresponding to Mb(H64V,V68A) (1).

1
2
3
4
5 To assess the impact of the cofactor and axial ligand substitution on the stability of the protein,
6 their apparent melting temperature (T_m) was determined via thermal denaturation experiments
7 using circular dichroism (CD) (**Figure 2** and **S2**). These studies revealed that incorporation of the
8 Fe(DADP) cofactor has no deleterious effect on the stability of the protein compared to heme-
9 containing counterpart ($T_m = 66.3^\circ\text{C}$ for Mb(H64V,V68A)[Fe(DADP)] (**2**) vs. 66.0°C for
10 Mb(H64V,V68A) (**1**)⁶⁰). Although substitution of the proximal His with N-methyl-histidine causes
11 a slight destabilization of the protein ($\Delta T_m = -2.9^\circ\text{C}$), the Mb(H64V,V68A,H93NMH)[Fe(DADP)]
12 (**3**) variant retains significant thermostability ($T_m = 63.4^\circ\text{C}$; **Figure 2**), indicating that both
13 structural modifications are well tolerated by the Mb scaffold.
14
15

16 The effect of these cofactor modifications on the $\text{Fe}^{3+}/\text{Fe}^{2+}$ reduction potential (E°) of the
17 metalloprotein was then investigated using a UV-vis spectrochemical method.⁶¹ For comparison
18 purposes, wild-type sperm whale Mb as well as a variant incorporating only the proximal ligand
19 substitution, Mb(H64V,V68A,H93NMH), were included in these analyses. As expected, these
20 experiments showed an shift of the redox potential toward more positive values for both the
21 Fe(DADP)- and NMH-containing variant ($E^\circ_{\text{Fe}^{3+}/\text{Fe}^{2+}} = 59 \pm 1$ mV and 77 ± 6 mV, respectively;
22 **Figure S3b-c**), compared to the parent protein Mb(H64V,V68A) (**1**) ($E^\circ_{\text{Fe}^{3+}/\text{Fe}^{2+}} = 54 \pm 1$ mV;
23 **Figure S3a**). Using the same spectrochemical assay, wild-type Mb was determined to have an E°
24 value of 47 ± 1 mV, which is very similar to those previously reported in the literature using other
25 methods.^{37,62} Notably, the combination of the Fe(DADP) cofactor with the NMH axial ligand leads
26 to a dramatic increase of the redox potential, resulting in a E° value of 146 ± 3 mV for the
27 Mb(H64V,V68A,H93NMH)[Fe(DADP)] (**3**) variant (**Figure S3d**). The nearly 100 mV increase
28 in E° for the latter variant compared to the +6 to +23 mV increases for the Fe(DADP)- and NMH-
29 containing variant, respectively, indicated a clear synergistic role of the non-native cofactor and
30 axial ligand toward affecting the redox potential of the metalloprotein.
31
32
33
34
35
36
37
38
39
40
41
42
43
44
45
46
47
48
49
50
51
52
53
54
55
56
57
58
59
60

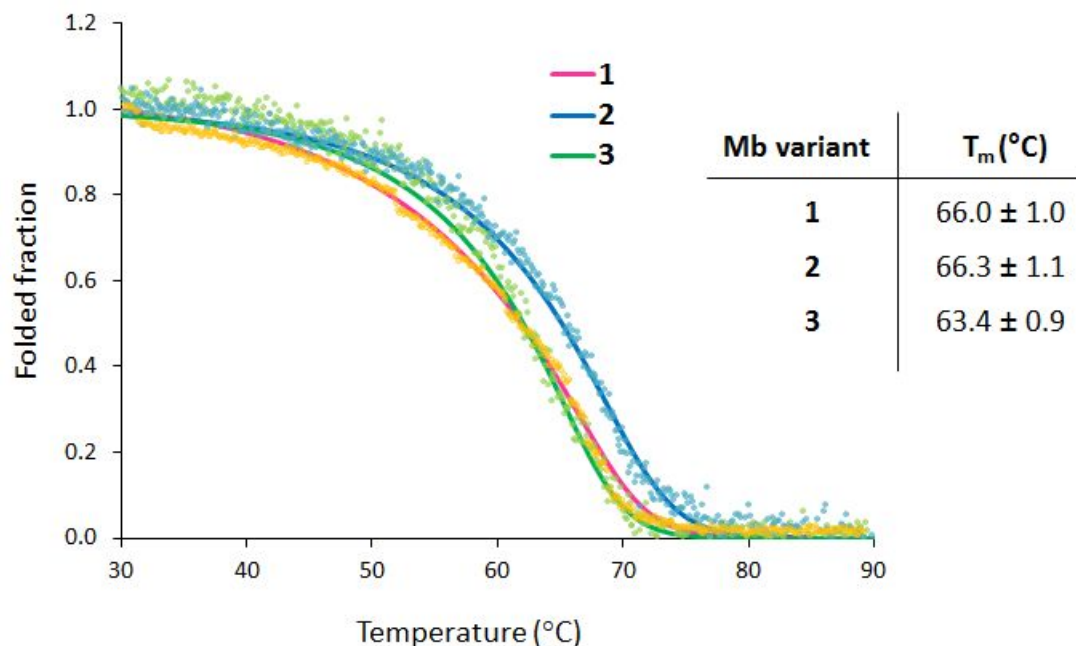


Figure 2. Thermal denaturation curves for Mb(H64V,V68A) (**1**), Mb(H64V,V68A)[Fe(DADP)] (**2**) and Mb(H64V,V68A,H93NMH)[Fe(DADP)] (**3**) as determined by circular dichroism (θ_{222}).

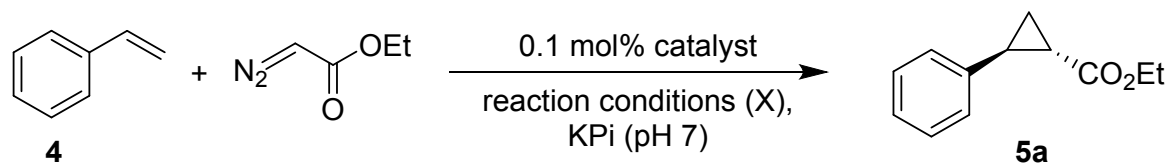
Cyclopropanation Activity

In order to evaluate the catalytic activity of Mb(H64V,V68A)[Fe(DADP)] (**2**) and Mb(H64V,V68A,H93NMH)[Fe(DADP)] (**3**) as cyclopropanation catalysts, these proteins were tested in a model reaction with styrene (**4**) and ethyl diazoacetate (EDA) under “standard reaction conditions” (10 mM styrene, 20 mM EDA, 10 mM sodium dithionite ($\text{Na}_2\text{S}_2\text{O}_4$), 0.1 mol% protein, anaerobic conditions). As summarized in **Table 1**, both proteins produce the desired product **5a** in quantitative yield and with excellent diastereo- and enantiomeric excess (>99% *de* and >98-99% *ee*; **Table 1**, Entry 2-3). The high cyclopropanation activity exhibited by Mb(H64V,V68A)[Fe(DADP)] (**2**) and Mb(H64V,V68A,H93NMH)[Fe(DADP)] (**3**) and the fact that both reactions proceed cleanly without the formation of carbene dimerization byproducts (diethyl maleate and fumarate) indicate that the [Fe(DADP)] cofactor can efficiently activate the diazo compound (EDA) promoting the carbene transfer reaction. In addition, both catalysts preserve the high stereoselectivity of the parent Mb(H64V,V68A) (**1**) variant, indicating that in either case the cofactor and cofactor/axial ligand substitution do not disrupt the active site structure of the protein.²⁹

1
2
3 Since modification of the porphyrin cofactor and/or proximal ligand can affect the sensitivity
4 of Mb-based carbene transferases to oxygen and/or non-reducing conditions,^{20, 21, 42, 47} the
5 cyclopropanation activity of the [Fe(DADP)]-based variants was also tested in the presence and in
6 the absence of oxygen and/or reductant (Na₂S₂O₄) (**Table 1** and **Table S1**). While the catalytic
7 activity of Mb(H64V,V68A) (**1**) decreases in the presence of oxygen (62% vs. >99% yield),
8 Mb(H64V,V68A,H93NMH)[Fe(DADP)] (**3**) maintains high cyclopropanation activity (85%
9 yield) under aerobic and reducing conditions (**Table 1**, Entry 6 vs. 4). This activity is higher than
10 in the presence of the Fe(DADP) cofactor or the His93NMH substitution alone (**Table S1**, Entry
11 3), indicating a combined effect of these substitutions toward increasing the oxygen tolerance of
12 the biocatalyst. Unlike Mb(H64V,V68A) (**1**), both [Fe(DADP)]-based variants and in particular
13 Mb(H64V,V68A,H93NMH)[Fe(DADP)] (**3**) exhibit high cyclopropanation activity (86-100%
14 yield) also under non-reducing (and anaerobic) conditions (**Table 1**, Entry 7-9).

15
16 As the [Fe(DADP)]-containing variants are prepared as ferric proteins, the catalytic activity
17 under non-reducing conditions can be explained based on the ability of these variants to undergo
18 *in situ* reduction by the EDA reagent to produce the catalytically active ferrous form⁴² or,
19 alternatively, by their ability to catalyze this reaction also in their ferric form, as previously
20 observed for an iron-chlorin e6 containing Mb variant.²¹ To gain insights into this aspect, the same
21 reactions were carried out in the presence of CO, which binds to the ferrous but not the ferric form
22 of these proteins as confirmed by UV-vis spectroscopy (**Figure 1b-c** and **Figure S4**). CO binding to
23 the iron center is expected to inhibit cyclopropanase activity. Under these conditions, the
24 cyclopropanation product **5a** was obtained only in trace amounts (**Table S1**, Entry 8). Control
25 experiments ruled out that CO-mediated reduction⁶³ of this protein occurs within a timescale
26 relevant for observation of cyclopropanation activity (i.e., <30-45 min) (**Figure S4**). These results
27 suggest that *in situ* generated ferrous form may contribute to the observed catalytic activity of the
28 Fe(DADP)-containing variants under non-reducing conditions. Given the lower activity of
29 Mb(H64V,V68A) (**1**) under these conditions, it is possible that the Fe(DADP) cofactor make these
30 variants susceptible to reduction by EDA, which can act as a mild reducing agent,⁶⁴⁻⁶⁷ a behavior
31 that may be at least in part attributed to their increased redox potential (E^o) compared to the heme-
32 containing parent protein.
33
34
35
36
37
38
39
40
41
42
43
44
45
46
47
48
49
50
51
52
53
54
55
56
57
58
59
60

Table 1. Catalytic activity of Mb(H64V,V68A) (**1**) and cofactor substituted variants thereof in the cyclopropanation of styrene with EDA.^a



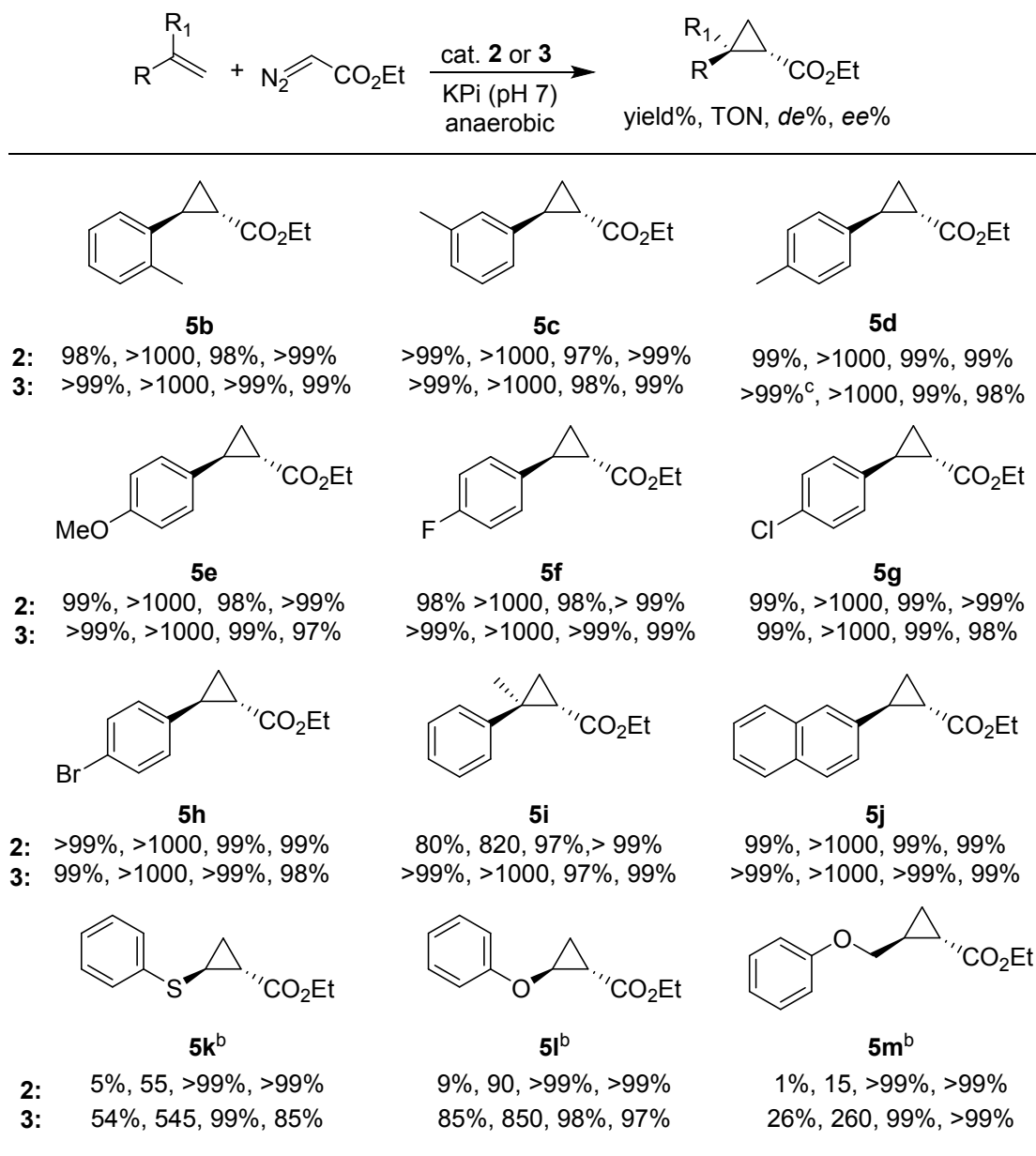
Entry	Catalyst	X ^b	Yield	TON	% <i>de</i>	% <i>ee</i>
1	1	-/red	>99%	>1000	>99	>99
2	2	-/red	>99%	>1000	>99	>99
3	3	-/red	>99%	>1000	>99	98
4	1	O ₂ /red	62%	620	>99	>99
5	2	O ₂ /red	39%	390	>99	>99
6	3	O ₂ /red	85%	850	>99	98
7	1	-/-	10%	150	>99	>99
8	2	-/-	86%	865	>99	>99
9	3	-/-	>99%	>1000	>99	>99
10	3	O ₂ /-	12%	125	>99	>99
11 ^c	3	-/-	>99%	2155	>99	>99
12 ^d	3	-/-	40%	4010	>99	>99

^a Reaction conditions: 10 mM styrene (**4**), 20 mM EDA, 10 μM purified Mb variant in KPi 50 mM (pH 7), r.t., 16 hours. Yield, diastereomeric and enantiomeric excess determined by chiral GC-FID analysis using 1,3-benzodioxole as internal standard. ^b Variable parameter (X): “-/red”=anaerobic, 10 mM Na₂S₂O₄; “-/-”=anaerobic, no reductant; “O₂/red”=aerobic, 10 mM Na₂S₂O₄; “O₂/-”=aerobic, no reductant. ^c Reaction performed using 5 μM protein. ^d Reaction performed using 1 μM protein.

Reactivity toward Aryl- and Heteroatom-Substituted Olefins

Based on the positive results from the studies above, we then assessed the catalytic performance of the Fe(DADP)-based variants toward the cyclopropanation of aryl-substituted olefins under non-reducing and anaerobic conditions. As shown in **Scheme 1**, a diverse panel of *para*-, *ortho*-, *meta*-, and α - substituted styrene derivatives were efficiently converted to the desired cyclopropanation products **5b-h** in good to excellent yield, and excellent *trans*-diastereoselectivity (98 to >99% *de*) and (1*S*,2*S*)-enantioselectivity (98% to >99% *ee*). Both electron-donating (**5b-e**) and electron-withdrawing groups (**5f-h**) in the phenyl ring were well tolerated. In addition, the sterically more demanding α -methylstyrene and 2-vinyl-naphtalene were also efficiently converted to the corresponding cyclopropane **5i** and **5j** with high diastereo- and enantioselectivity. Moreover, unlike Mb(H64V,V68A)[Fe(DADP)] (**2**), Mb(H64V,V68A,H93NMH)[Fe(DADP)] (**3**) showed also good activity toward non-styrenyl substrates such as phenylvinylether and phenylvinylsulfane, producing **5k**, and **5l**, respectively, in good to high yield and with high stereoselectivity. The number of catalytic turnovers (TON) observed with these substrates are 2- to 3-fold higher than those obtained with Mb(H64V,V68A) (**1**) under reducing conditions. The unactivated olefin substrate (allyloxy)benzene was also converted by Mb(H64V,V68A,H93NMH)[Fe(DADP)] (**3**) into the cyclopropane product **5m**. In this case, the Fe(DADP)-based catalyst also offers improved stereoselectivity (>99% *de* and *ee*) compared to the parent enzyme (95% *de*, 86% *ee*).

Scheme 1. Substrate scope of Mb(H64V,V68A)[Fe(DADP)] (**2**) and Mb(H64V,V68A,H93NMH)[Fe(DADP)] (**3**).^a



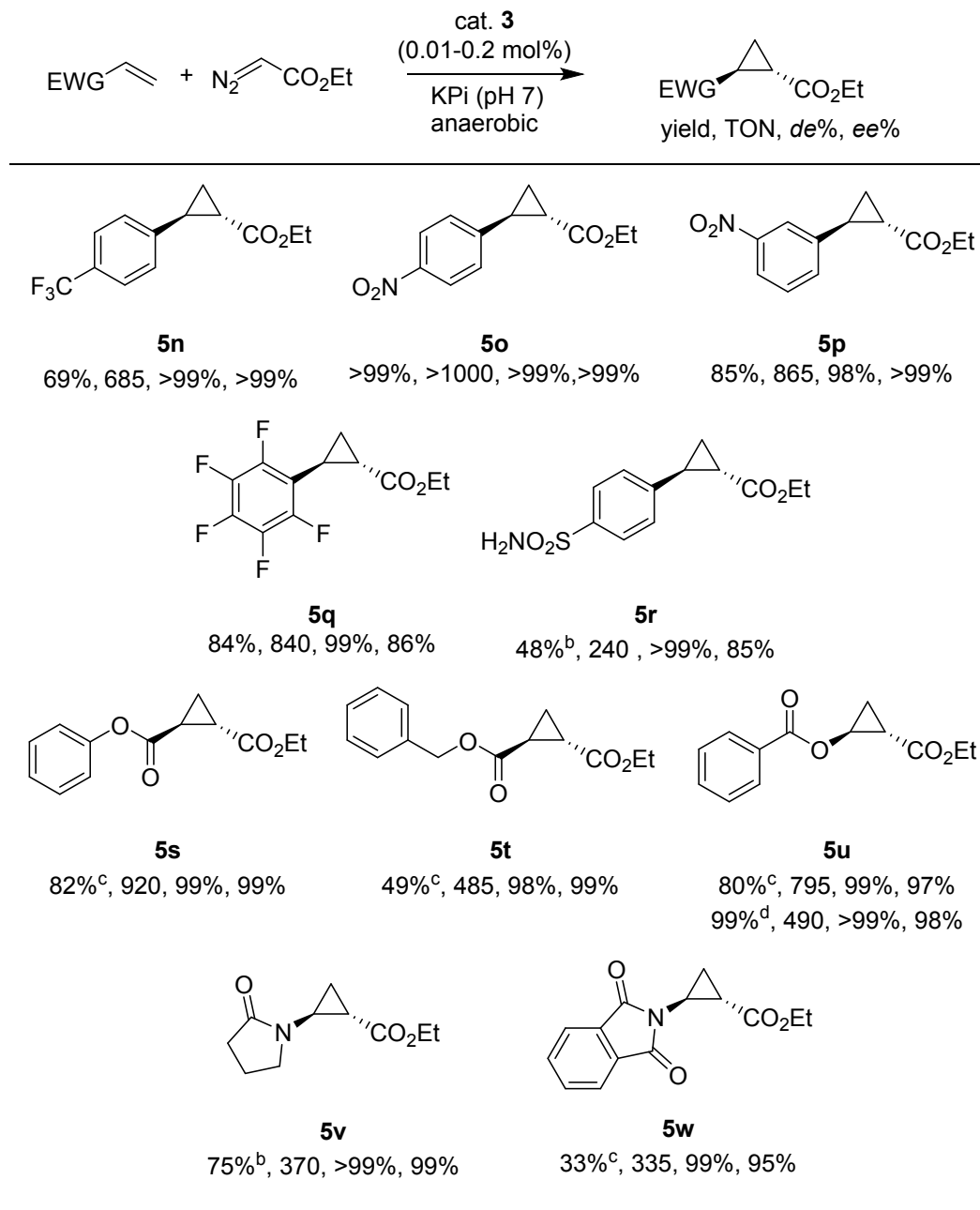
^a Reaction conditions: 10 mM alkene, 20 mM EDA, 10 μ M Mb variant **2** or **3** in KPi buffer (50 mM, pH 7), r.t., 16 hrs, anaerobic conditions. Yield and diastereomeric excess were determined by chiral GC-FID analysis. Enantiomeric excess was determined by chiral GC-FID or SFC analysis. ^b 50 mM alkene, 20 mM EDA, 20 μ M catalyst **3**.

Stereoselective Cyclopropanation of Electron-Deficient Olefins

The high cyclopropanation activity of Mb(H64V,V68A,H93NMH)[Fe(DADP)] (**3**) toward the monohalogenated styrenes (products **5f**, **5g**, and **5h** in **Scheme 1**) was in line with our goal of enhancing the reactivity of Mb-based systems toward electron-poor olefins and encouraged us to assess its scope toward more challenging substrates such as trifluoromethyl-, nitro-, and pentafluoro-styrenes (**Scheme 2**). Gratifyingly, the corresponding cyclopropanation products **5n-q** could be obtained in high (69-85%) to quantitative yield (**5o**), along with high diastereo- and enantioselectivity (98 to >99% *de*; 86 to >99% *ee*). Notably, 4-vinylbenzenesulfonamide, whose cyclopropanation failed using Mb(H64V,V68A) (**1**) or commonly adopted organometallic carbene transfer catalysts such as Rh₂(OAc)₄ and Fe(TPP)Cl (**Table S2**), was successfully cyclopropanated in the presence of Mb(H64V,V68A,H93NMH)[Fe(DADP)] (**3**) to afford **5r** in 48% yield and >99% *de* and 84% *ee* (**Scheme 2**).

Mb(H64V,V68A,H93NMH)[Fe(DADP)] (**3**) could be successfully applied to the stereoselective cyclopropanation of a variety of other electron-deficient non-styrenyl olefins. While acrylate esters are notoriously challenging substrates for transition metal-catalyzed cyclopropanation,^{52, 68} phenyl and benzyl acrylate could be converted to the desired products **5s** and **5t**, respectively, in good to high yields (49-89%) and high enantiopurity (98-99% *de*; 99% *ee*). Vinyl benzoate, which is unreactive in the presence of Fe(TPP)Cl and Mb(H64V,V68A) (**1**) and only poorly reactive toward Rh₂(OAc)₄ (**Table S3**), was also efficiently cyclopropanated by Mb(H64V,V68A,H93NMH)[Fe(DADP)] (**3**) to give enantiopure **5u** in quantitative yield with 99% *de* and 97% *ee*. Time-course experiments showed this reaction proceeds rapidly, with >90% of the final product being formed within the first 10 minutes and that it is faster than the cyclopropanation of styrene (**Figure S5**). It is also worth noting that this transformation can provide an expedite route (i.e., via hydrolysis of **5u**) to cyclopropanols, which are valuable building blocks for drug synthesis. Finally, the Mb(H64V,V68A,H93NMH)[Fe(DADP)]-catalyzed cyclopropanation of N-vinyl-amides and succinamides was also successful, affording the corresponding cyclopropanes **5v** and **5w** in good to moderate yields (75-33%) and high stereoselectivity. Comparable selectivity but somewhat reduced yield (by 20-30%) were obtained for the Mb(H64V,V68A,H93NMH)[Fe(DADP)]-catalyzed reactions with the electrondeficient olefins in the presence of sodium dithionite, indicating an optimal performance of this catalyst under non-reducing conditions.

Scheme 2. Mb(H64V,V68A,H93NMH)[Fe(DADP)]-catalyzed cyclopropanation of electrondeficient olefins.^a



^a Reaction conditions: 10 mM alkene, 20 mM EDA, 10 μ M catalyst **3** in KPi buffer (50 mM, pH 7), r.t., 16 hrs, anaerobic conditions. Yield and diastereomeric excess were determined by chiral GC-FID analysis. Enantiomeric excess was determined by chiral GC-FID or SFC analysis. ^b 20 mM alkene, 10 mM EDA, 20 μ M **3**. ^c 50 mM alkene, 20 mM EDA, 20 μ M **3**. ^d 2.5 mM alkene, 2.5 mM EDA, 5 μ M **3**.

1
2
3 In general, Mb(H64V,V68A)[Fe(DADP)] (**2**) and Mb(H64V,V68A,H93NMH) proved to be
4 inferior catalysts for the cyclopropanation of the electrodeficient alkenes compared to
5 Mb(H64V,V68A,H93NMH)[Fe(DADP)] (**3**). For example, cyclopropane **5r** and **5u** were obtained
6 in <20% yields using either of these catalysts compared to 50-80% yields obtained with
7 Mb(H64V,V68A,H93NMH)[Fe(DADP)] (**3**) under the same reaction conditions (**Tables S2** and
8 **S3**). Mirroring the observed effect on other functional properties (i.e. E^0 , sensitivity to
9 reductant/oxygen), these results point at a synergistic effect of the Fe(DADP) cofactor and axial
10 *N*-methyl-histidine ligand toward conferring high reactivity toward these challenging substrates.
11
12
13
14
15
16
17
18

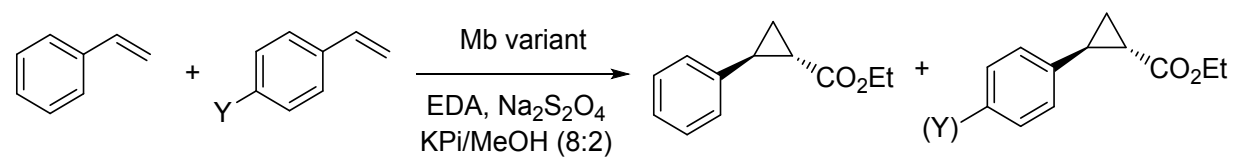
19 Mechanistic Studies

20 To gain insights into the mechanistic basis for the divergent reactivity of
21 Mb(H64V,V68A,H93NMH)[Fe(DADP)] (**3**) compared to His-ligated heme counterpart, we
22 measured the relative rates of these catalysts for the cyclopropanation of a series of *para*-
23 substituted styrenes vs. styrene via competition experiments. Consistent with our previous
24 observations,⁹ styrene derivatives carrying electron-donating groups (i.e., -Me, -OMe) showed
25 higher reactivity than styrene in the Mb(H64V,V68A)-catalyzed reactions, whereas electron-
26 deficient styrenes (e.g., *p*-CF₃, *p*-NO₂) exhibited reduced cyclopropanation rates compared to
27 styrene (**Table 2, Figure S6**). Plots of the corresponding $\log(k_X/k_H)$ values against the Hammett
28 constants⁶⁹ σ_p and σ^+ gave relatively good linear correlations, yielding a ρ_p value of -1.2 ($R^2 =$
29 0.84) and a ρ^+ value of -0.77 ($R^2 = 0.77$), respectively (**Figure 3a**). Similar plots generated after
30 excluding *p*-bromo-styrene, which showed the largest deviation from the trend, yielded even
31 stronger linear correlations ($R^2 = 0.88-0.93$) without affecting the ρ values ($\rho_p = -1.2$; $\rho^+ = -0.79$).
32 The large negative ρ values is consistent with the electrophilic nature of the metal carbene
33 intermediate involved in these reactions.^{9,27}
34
35
36
37
38
39
40
41
42
43
44

45 In stark contrast to the reactivity trend exhibited by Mb(H64V,V68A) (**1**), the rate of
46 Mb(H64V,V68A,H93NMH)[Fe(DADP)]-catalyzed cyclopropanation is accelerated by the
47 presence of electron-withdrawing groups in the styrene substrates, whereas reduced
48 cyclopropanation rates are observed with the electron-rich styrenes relative to unsubstituted
49 styrene (**Table 2, Figure S7**). The corresponding $\log(k_X/k_H)$ values showed no correlation with the
50 polar substituent constant σ_p or σ^+ ($R^2 = 0.07-0.1$) (**Figure 3b**). The non-linearity of these plots,
51 along with our previous observations concerning the radical mechanism of hemoprotein-catalyzed
52
53
54
55
56
57
58
59
60

nitrene transfer reactions,⁷⁰ prompted to us to consider the potential involvement of intermediates with significant radical character in Mb(H64V,V68A,H93NMH)[Fe(DADP)]-catalyzed cyclopropanation.

Table 2. Relative rates scales for the cyclopropanation of *para*-substituted styrene catalyzed by Mb(H64V,V68A) (**1**) and Mb(H64V,V68A,H93NMH)[Fe(DADP)] (**3**) and sigma and sigma-dot scales for *para* substituents.^a



Substituent	k_X/k_H (catalyst 1)	k_X/k_H (catalyst 3)	σ_p	σ^+	σ_{mb}	σ^*_{JJ}
-OMe	1.04	0.65	-0.27	-0.778	-0.77	0.23
-Me	0.61	0.89	-0.17	-0.31	-0.29	0.15
-Cl	0.39	1.12	0.23	0.11	0.11	0.22
-Br	0.66	1.39	0.23	0.15	0.13	0.23
-CF ₃	0.16	0.28	0.54	0.61	0.49	-0.01
-NO ₂	0.04	3.43	0.78	0.79	0.86	0.36

^a σ_p and σ_p are the Hammett constants⁶⁹ and σ_{mb} and σ^*_{JJ} are Jiang's polar⁷¹ and spin-delocalization constants⁷², respectively, for *para*-substituted aryl derivatives.

Supporting this hypothesis, a very good linear correlation ($R^2 = 0.86$) was obtained between the $\log(k_X/k_H)$ values and Jiang's spin-delocalization substituent constants σ^*_{JJ} ⁷² (**Figure 3c**; **Table 3**). An even stronger correlation ($R^2 = 0.93$) was achieved using the dual-parameter equation $\log(k_X/k_H) = \rho^X\sigma^X + \rho^*\sigma^*$, which takes into consideration of both the polar (σ^X) and spin-delocalization effects (σ^*) of the substituents.⁷³⁻⁷⁵ Fitting of this equation to the data via multiple linear regression using Jiang's σ_{mb} ⁷¹ polar scale and σ^*_{JJ} ⁷² radical scale yielded a ρ_{mb} and ρ^*_{JJ} value of 0.18 and 2.6, respectively (**Figure 3d**, **Table 3**). While the improved correlation achieved with the extended equation compared to the radical scale alone suggests the participation of both polar

and spin effects in affecting the rate of the reaction, the small $\rho_{\text{mb}}/\rho_{\text{JJ}}^{\bullet}$ ratio of 0.06 indicates a dominance of the spin-delocalization effect over the polar effect.⁷⁵ In stark contrast, dual-parameter fitting of the Mb(H64V,V68A) (**1**) data yielded a large negative σ_{mb} (-0.79 vs. +0.18 for **3**; **Table 3**) and a $\rho_{\text{mb}}/\rho_{\text{JJ}}^{\bullet}$ above the unity (= 1.5), which have been attributed to reactions dominated by polar effects.⁷⁵

Table 3. Rho and R² values for single- and dual-parameters correlations of log(k_X/k_H) values for Mb(H64V,V68A) (**1**) and Mb(H64V,V68A,H93NMH)[Fe(DADP)] (**3**) with sigma and sigma-dot parameters. N.a. = not applicable due to non-linear correlation.

Catalyst	Parameters	ρ^{X}	ρ_{mb}	$\rho_{\text{JJ}}^{\bullet}$	$ \rho_{\text{mb}}/\rho_{\text{JJ}}^{\bullet} $	R ²
1	σ_{p}	-1.2	-	-	-	0.84
1	σ^{+}	-0.77	-	-	-	0.77
1	$\sigma_{\text{JJ}}^{\bullet}$	-	-	n.a.	-	0.05
1	$\sigma_{\text{mb}}/\rho_{\text{JJ}}^{\bullet}$	-	-0.79	-0.52	1.5	0.84
3	σ_{p}	n.a.	-	-	-	0.10
3	σ^{+}	n.a.	-	-	-	0.07
3	$\sigma_{\text{JJ}}^{\bullet}$	-	-	2.7	-	0.86
3	$\sigma_{\text{mb}}/\sigma_{\text{JJ}}^{\bullet}$	-	0.18	2.6	0.06	0.93

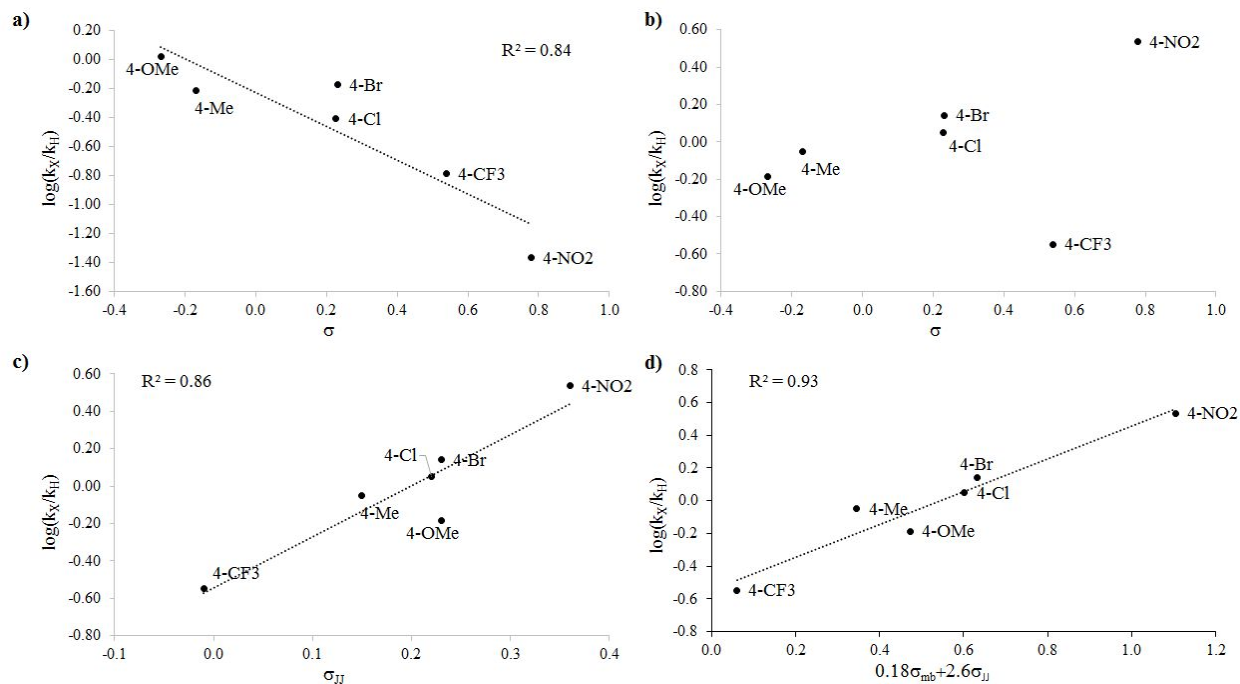


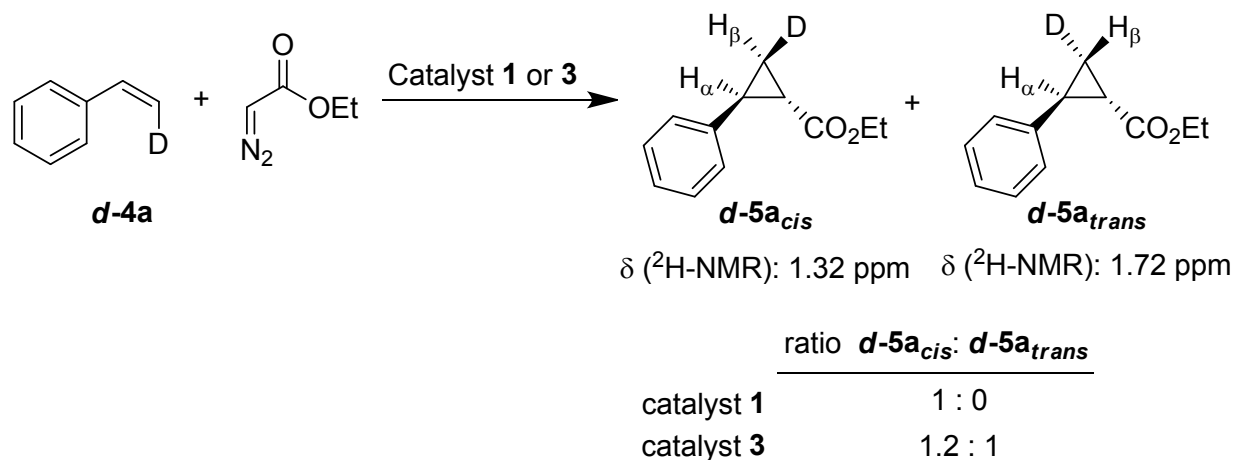
Figure 3. Hammett plots. (a) Plot of $\log(k_X/k_H)$ for Mb(H64V,V68A) (**1**) vs. σ constant. (b-d) Plots of $\log(k_X/k_H)$ for Mb(H64V,V68A,H93NMH)[Fe(DADP)] (**3**) vs. σ constant (b), σ_{JJ} constant (c) and $0.18\sigma_{mb} + 2.6\sigma_{JJ}$ (d).

To further probe the occurrence of a radical mechanism in the Mb(H64V,V68A,H93NMH)[Fe(DADP)]-catalyzed cyclopropanation process, reactions were carried out using EDA and the isotopically labelled substrate *cis*- β -deuterostyrene (**d-4a**) (see Experimental details), where a (partial) loss of stereospecificity would reveal the occurrence of a radical intermediate. Insightfully, this reaction led to the formation of **d-5a** in low yield as a 1.2:1 mixture of *cis* and *trans* isomers with respect to the -D and -Ph groups, as determined based on ¹H and ²H NMR spectra (**Scheme 3**). In contrast, the same reaction in the presence of Mb(H64V,V68A) (**1**) proceeds stereospecifically with no scrambling of the deuterium label. In comparison, ~40% isomerization was observed for the same reaction using Co(TPP) as the catalyst,²⁷ a result in line with the radical cyclopropanation mechanism previously established for this system.^{76, 77} Altogether, these experiments provided strong evidence for the intermediacy of a radical intermediate in the Mb(H64V,V68A,H93NMH)[Fe(DADP)] (**3**) reaction.

To further corroborate this conclusion, the Mb(H64V,V68A,H93NMH)[Fe(DADP)]-catalyzed reaction with styrene and EDA was carried out in the presence and in absence of the

1
2
3 radical spin trapping agents 5,5-dimethyl-1-pyrroline N-oxide (DMPO) (**Table 4**). In the presence
4 of DMPO, a significant reduction (by 58%) in the yield of the cyclopropane product **5a** was
5 observed under reducing conditions compared to a parallel reaction lacking the spin trapping agent
6 (Entry 7 vs. 6). A similar effect but with a higher degree of inhibition (77% reduction in yield) was
7 observed under non-reducing conditions. Very similar results were obtained from parallel
8 experiments involving 4-hydroxy-2,2,6,6-tetramethylpiperidin-1-oxyl (TEMPO) in place of
9 DMPO as the spin trapping agent (**Table 4**, Entries 3 and 8). In contrast, the Mb(H64V,V68A)-
10 catalyzed cyclopropanation reaction showed only a small reduction in yield upon addition of
11 DMPO or TEMPO (**Table 4**, Entries 2-3 vs. 1). In line with these results, kinetic experiments
12 showed a drastic reduction of the cyclopropanation rate of
13 Mb(H64V,V68A,H93NMH)[Fe(DADP)] (**3**) in the presence of DMPO compared to a reaction
14 without it (38 vs. 670 turnovers min⁻¹), whereas the cyclopropanation rate of Mb(H64V,V68A) (**1**)
15 was only minimally affected by the spin trapping agent (510 vs. 550 turnovers min⁻¹; **Figure S10**).
16
17

18 To probe the step at which DMPO-mediated inhibition occurs, inhibition experiments were
19 performed in the presence of EDA but in the absence of styrene, under which conditions the
20 carbene dimerization products diethyl malonate/maleate are produced. Insightfully, nearly full
21 suppression (>95%) of the carbene dimerization product was observed in the presence of DMPO
22 with Mb(H64V,V68A,H93NMH)[Fe(DADP)] (**3**) (**Table 4**, Entry 10 vs. 9), whereas only little
23 inhibition (<20%) was observed with Mb(H64V,V68A) (**1**) (**Table 4**, Entry 5 vs. 4). Taken
24 together, the Hammett analyses and radical rearrangement/trapping experiments converged in
25 supporting (a) the occurrence of a step-wise radical-based mechanism for the
26 Mb(H64V,V68A,H93NMH)[Fe(DADP)]-catalyzed olefin cyclopropanation reaction and (b) the
27 intermediacy of a metallocarbene species with significant radical character, as evidenced by its
28 susceptibility to inhibition by spin trapping agents.
29
30
31
32
33
34
35
36
37
38
39
40
41
42
43
44
45
46
47
48
49
50
51
52
53
54
55
56
57
58
59
60

Scheme 3. Enzymatic cyclopropanation reactions with *cis*- β -deuterostyrene (**d-4a**).**Table 4.** Inhibition experiments with spin trapping agents in styrene cyclopropanation reaction catalyzed by Mb(H64V,V68A) (**1**) or Mb(H64V,V68A,H93NMH)[Fe(DADP)] (**3**).^a

Entry	Catalyst	Styrene	Inhibitor	Yield	% <i>de</i>	% <i>ee</i>
1	1	Yes	None	>99%	99	>99
2	1	Yes	DMPO	89%	99	>99
3	1	Yes	TEMPOL	90%	>99	99
4	1	No	None	95% ^b	-	-
5	1	No	DMPO	80% ^b	-	-
6	3	Yes	None	>99%	>99	>99
7	3	Yes	DMPO	42%	>99	99
8	3	Yes	TEMPOL	40%	>99	99
9	3	No	None	88% ^b	-	-
10	3	No	DMPO	8% ^b	-	-

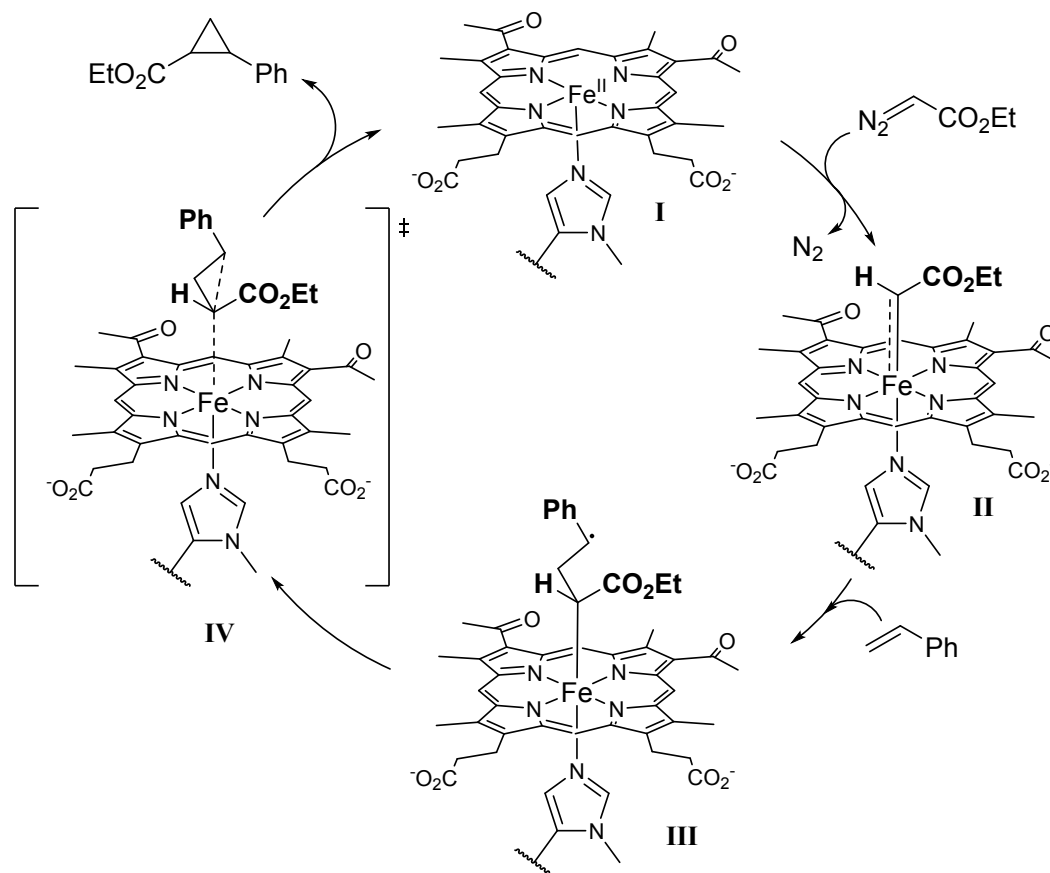
^a Reaction conditions: 10 mM styrene, 20 mM EDA, 100 mM DMPO (or TEMPOL), 20 μM Mb variant, 10 mM sodium dithionite in 50 mM potassium phosphate buffer (pH 7) containing 10% DMF, r.t., 16 hours. Yield, diastereomeric and enantiomeric excess were determined by chiral GC-FID analysis. ^b Yield of diethyl malonate and maleate determined by chiral GC-FID analysis.

1
2
3 On the basis of these results, a plausible mechanism for this reaction is proposed in **Scheme**
4 **4**. Under reducing conditions, the ferrous form of the protein (**I**) reacts with the diazo reagent to
5 form an iron-bound carbene intermediate (**II**). While the structural and electronic features of this
6 species awaits further elucidation, this intermediate clearly possesses distinct reactivity compared
7 to the heme-bound carbene intermediate²⁷ and possesses significant radical character, as evidenced
8 by its reactivity toward the radical trapping agent. Upon generation of this species, metallocarbene-
9 radical activation of the olefin substrates is envisioned to ensue, leading to a carbon-centered
10 radical intermediate (**III**). Ring closure leads to the cyclopropane product and regenerates the
11 catalyst (**Scheme 4**).

12
13 Under non-reducing conditions, a similar mechanism may be operative after generation of the
14 catalytically competent ferrous form via *in situ* reduction of the ferric protein by the diazo
15 compound. This reductive process could be facilitated by the increase in the redox potential
16 associated with the incorporation of NMH-ligated Fe(DADP) cofactor compared to the histidine-
17 ligated heme counterpart. While the CO inhibition experiments would support this hypothesis, a
18 cyclopropanation pathway mediated by the ferric form of this protein is also considered viable.
19 Fe(III)-based catalysts capable of promoting cyclopropanation reactions have been described^{67, 78-}
20 ⁸¹ and we previously reported a Mb variant functioning as cyclopropanase in its ferric state.²¹ This
21 alternative scenario is suggested by various pieces of experimental data, including the higher
22 cyclopropanation activity of Mb(H64V,V68A,H93NMH)[Fe(DADP)] (**3**) with the
23 electrondeficient olefins and the higher degree of DMPO-induced inhibition observed under non-
24 reducing vs. reducing conditions. Future studies are warranted to elucidate these aspects in more
25 detail.

26
27
28
29
30
31
32
33
34
35
36
37
38
39
40
41
42
43
44
45
46
47
48
49
50
51
52
53
54
55
56
57
58
59
60

Scheme 4. Proposed mechanism for Mb(H64V,V68A,H93NMH)[Fe(DADP)]-catalyzed cyclopropanation reaction.



Further Discussion

The radical-based stepwise mechanism operating in the present system is reminiscent of that reported for olefin cyclopropanation catalyzed by Zhang and de Bruin's Co-porphyrins^{76,77} and an open-shell iron alkylidene complex recently reported by Deng and coworkers,⁸² both of which systems were found to be reactive toward electron-deficient alkenes.^{52, 82} The reactivity of the Fe(DADP)-based biocatalyst **3** toward electron-poor olefins (**Scheme 2**) sets it apart from the electrophilic reactivity of Fisher-type metallocarbenes involved in cyclopropanation reactions catalyzed by Mb ($\rho = -1.2$; **Figure 3a**) and various organometallic catalysts, including iron- ($\rho = -0.68^{65}$; $\rho^+ = -0.41^{83}$), ruthenium- ($\rho^+ = -0.44^{84}$), and iridium-porphyrins ($\rho^+ = -0.22^{85}$),

1
2
3 mononuclear Rh ($\rho^+ = -0.40^{86}$) and copper complexes ($\rho = -0.85^{87}$; $\rho^+ = -0.76^{86}$; $\rho^+ = -0.74^{88}$).
4
5 Furthermore, the positive ρ_{mb} value (0.18), along with the large ρ^*_{JJ} (2.6), obtained for the
6
7 Fe(DADP)-based catalyst suggest the involvement of a metallocarbene radical intermediate with
8
9 some nucleophilic character. Such characteristics, which arise from a synergistic role of the
10
11 Fe(DADP) cofactor and NMH axial ligand, can explain the expanded substrate scope of the
12
13 cofactor engineered biocatalyst toward electron-poor (**5n-5w**; **Scheme 2**) and unactivated olefins
14
15 (**5m**; **Scheme 1**) in addition to electron-rich alkenes (**5a-5l**; **Scheme 1**).

16
17 As supported by our results, reconfiguration of the first coordination sphere around the iron
18
19 center via the porphyrin and axial ligand substitutions induces a dramatic change in the mechanism
20
21 of the intermolecular olefin cyclopropanation investigated here, going from a (predominantly)
22
23 concerted carbene transfer process dominated by polar effects and mediated by an electrophilic
24
25 heme-carbene intermediate,²⁷ to a stepwise radical mechanism dominated by spin delocalization
26
27 effects and mediated by a metallocarbene intermediate with radical-type, dual
28
29 nucleophilic/electrophilic character. While ligand-induced changes in reaction mechanisms have
30
31 been in some cases observed for transition metal-catalyzed transformations,^{89, 90} this is the first
32
33 instance, to the best of our knowledge, where this effect is achieved in the context of a
34
35 metalloprotein.

36
37 It should be further noted that we previously observed a latent radical reactivity of free hemin
38
39 in intermolecular cyclopropanation reactions with EDA (2% isomerization with β -
40
41 deuterostyrene)²⁷, whereas more recent studies from our laboratory showed evidence for the
42
43 occurrence of radical-mediated rearrangements in Mb-catalyzed intramolecular cyclopropanation
44
45 reactions.⁹¹ Based on this knowledge and the present work, we set forth the hypothesis that
46
47 hemoproteins may possess a dual (or multistate) reactivity in carbene transfer reactions, possibly
48
49 involving distinct intermediates and reaction pathways, akin to that proposed for metal- and
50
51 metalloenzyme-catalyzed oxo transfer processes.^{92, 93} Importantly, the present studies demonstrate
52
53 how modification of the first coordination sphere around the iron can provide an effective strategy
54
55 for enhancing the radical-type carbene transfer reactivity of this system, enabling cyclopropanation
56
57 reactions not readily accessible using their native cofactor-containing counterparts. Further studies
58
59 are warranted to elucidate the nature of the catalytic intermediates involved in these reactions and
60
61 better understand the role played by the cofactor/axial ligands in favouring the observed radical-
62
63 type reactivity, which is only rarely found among organometallic carbene transfer catalysts.^{76, 82}

Conclusion

In summary, we have described the design and development of a metalloprotein catalyst useful for the stereoselective cyclopropanation of both electron-rich and electron-poor alkenes. A variety of electrondeficient styrenes and alkenes, which are either poorly reactive or unreactive toward heme-based protein catalysts, were effectively cyclopropanated by this system with high catalytic activity as well as high diastereo- and enantioselectivity. Our mechanistic studies show that the expanded reaction scope of this biocatalyst compared to the heme-based counterpart is dependent upon the acquisition of radical-type carbene transfer reactivity as a result of the reconfigured primary coordination sphere around the iron center through a N-methyl-histidine-ligated Fe(DADP) cofactor. Hammett analyses and radical rearrangement/trapping experiments provide evidence for the involvement of a radical-based, stepwise mechanism in these reactions, which differs from the concerted nonsynchronous carbene transfer mechanism previously found to dominate Mb- and iron-porphyrin-catalyzed intermolecular cyclopropanations with diazoesters.^{94, 95} This study highlights the value of cofactor engineering for tuning the reactivity and expanding the reaction scope of metalloproteins in the context of abiological reactions. Furthermore, in view of the unique and attractive features of radical-mediated reactions,⁹⁶⁻⁹⁹ the metallocarbene radical reactivity exhibited by the present system is expected to prove useful in the context of other synthetically valuable transformations.

EXPERIMENTAL DETAILS

General Information. All chemicals and reagents were purchased from commercial suppliers (Sigma-Aldrich, Alfa Aesar, Frontier Scientific Inc, Chem-Impex Int.) and use without any further purification, unless otherwise stated. All dry reactions were carried out under argon pressure in oven-dried glassware with magnetic stirring using standard gas-tight syringes, cannula, and septa. ^1H and ^{13}C NMR spectra were measured on a Bruker DPX-400 instrument (operating at 400MHz for ^1H , 100 MHz for ^{13}C) or a Bruker DPX- instrument (operating at 500 MHz for ^1H and 125 MHz for ^{13}C). Column chromatography purification was carried out using AMD Silica Gel 60 230-400 mesh. Thin Layer Chromatography (TLC) was carried out using Merck Millipore TLC silica gel 60 F254 glass paltes. Gas chromatography (GC) analyses were carried out using a Shimadzu GC-2010 gas chromatograph equipped with a FID detector, and a Cyclosil-B column (30 m x 0.25 mm x 0.25 μm film). Supercritical Fluid Chromatography (SFC) analysis were performed using a JASCO Analytical and Semi-Preparative SFC instrument equipped with a column oven (35 $^\circ\text{C}$), photodiode array detector, a backpressure regulator (12.0 MPa), a carbon dioxide pump and a sample injection volume of 3 μL .

Synthetic Procedures. Detailed procedures for the synthesis of $\text{Fe}(\text{DADP})\text{Cl}$, *cis*- β -deuterostyrene and cyclopropanes **5a-w** are provided in the Supporting Information.

Growth Media. Cell cultures were grown in enriched M9 medium which was prepared follows. For 1 L, 779 mL deionized H_2O were mixed with 200 mL M9 salts (5X) solution, 10 mL casamino acids (20% m/v), 10 mL glycol, 1 mL MgSO_4 (2M), and 100 μL CaCl_2 (1M). The M9 (5X) solution was prepared by dissolving 15 g Na_2HPO_4 , 7.5 g K_2HPO_4 , 2.5 g NaCl , 5 g NH_4Cl in 1 L deionized H_2O and sterilized by autoclaving. The casamino acids, glycol and MgSO_4 solutions were autoclaved separately. The CaCl_2 solution was sterilized by filtration. Enriched M9 agar plates were prepared by adding 17 g agar to 1 L of enriched M9 media containing all of the aforementioned components at the specified concentrations with the exception of CaCl_2 , which was added immediately prior to plating. To media and plates, ampicillin was added to a final concentration of 100 mg/L and chloramphenicol was added to a final concentration of 34 mg/L.

1
2
3 **Protein Expression.** Cloning of MbH64V,V68A was described previously.⁹
4 Mb(H64V,V68A) was expressed in *E.coli* C41(DE3) cells as follows. After transformation, cells
5 were grown in TB medium (ampicillin, 100 mg/L) at 37°C (200 rpm) until OD₆₀₀ reached 0.6.
6 Cells were then induced with 0.25 mM isopropyl-β-D-1-thiogalactopyranoside (IPTG) and 0.3
7 mM γ-aminolevulinic acid (ALA). After induction, cultures were shaken at 180 rpm and 27 °C
8 and harvested after 20 h by centrifugation at 4,000 rpm at 4°C. The cells were resuspended in 20
9 mL of Ni-NTA Lysis Buffer (50 mM KPi, 250 mM NaCl, 10 mM histidine, pH 8.0). Resuspended
10 cells were frozen and stored at -80°C until purification.
11
12
13
14
15
16
17

18 **Expression of Cofactor-Substituted Myoglobin variants.** Mb(H64V,V68A)Fe(DADP)
19 was expressed in *E.coli* C41(DE3) cells using pET22_Mb(H64V,V68A) as follows. The cells were
20 plated on a lysogeny broth agar plate containing ampicillin and a single colony of freshly
21 transformed cells was cultured in 5 mL of lysogeny broth medium containing ampicillin. The
22 overnight cultures were transferred to 1 L enriched M9 medium containing ampicillin, followed
23 by incubation at 37°C with shaking (180 rpm). At OD₆₀₀ of 1.4, cells were induced with 0.25 mM
24 IPTG and the induced culture was shaken at 27°C and rpm 180 for additional 16 to 20 hours. After
25 harvesting, the cells were pelleted by centrifugation, resuspended in 20 mL of Ni- NTA Lysis
26 Buffer (50 mM KPi, 250 mM NaCl, 10 mM histidine, pH 8.0) and 20 μL of a cofactor solution
27 (30 mg/mL in DMF) were added. Cells were lysed by sonication and the cell lysate was clarified
28 by centrifugation (14,00 rpm, 4°C, 30 min). For expression of
29 Mb(H64V,V68A,H93NMH)Fe(DADP), pET29b_Mb(H64V,V68A,H93NMH) and pEVOL-
30 PyIRS(NMH) were used to transform *E.coli* BL21(DE3) and the cells were plated on a lysogeny
31 broth agar plate containing ampicillin and chloramphenicol. A single colony of freshly transformed
32 cells was cultured overnight in 5 mL of lysogeny broth medium containing ampicillin and
33 chloramphenicol. The overnight cultures were transferred to 1 L enriched M9 medium containing
34 ampicillin and chloramphenicol, followed by incubation at 37°C with shaking (180 rpm). At OD₆₀₀
35 of 0.4, cell cultures were condensed by centrifugation (4,000 rpm, 4°C, 30 min) followed by
36 resuspension of the cell pellets in 200 mL of enriched M9 medium. To the condensed expression
37 cultures, N-3-methyl-L-histidine (NMH) and arabinose were added to a final concentration of X
38 mM and X mM, respectively, and then cultures were shaken at 24°C and 180 rpm for 20 minutes
39 before induction with 0.25 mM IPTG. The induced culture was shaken at 24°C and rpm 180 for
40 additional 16 to 20 hours. After harvesting, the cells were pelleted by centrifugation, resuspended
41
42
43
44
45
46
47
48
49
50
51
52
53
54
55
56
57
58
59
60

1
2
3 in 20 mL of Ni-NTA Lysis Buffer (50 mM KPi, 250 mM NaCl, 10 mM histidine, pH 8.0) and 20
4 μ L of a cofactor solution (30 mg/mL in DMF) were added. Cells were lysed by sonication and the
5 cell lysate was clarified by centrifugation (14,00 rpm, 4°C, 30 min).
6
7

8
9 **Protein Purification.** The clarified lysate was transferred to a Ni-NTA column
10 equilibrated with Ni-NTA Lysis Buffer. The resin was washed with 50 mL of Ni-NTA Lysis Buffer
11 and then 50 mL of Ni-NTA Wash Buffer (50 mM KPi, 250 mM NaCl, 20 mM histidine, pH 8.0).
12 Proteins were eluted with Ni-NTA Elution Buffer (50 mM KPi, 250 mM NaCl, 250 mM histidine,
13 pH 7.0). After elution from the Ni-NTA column, the protein was buffer exchanged against 50 mM
14 KPi buffer (pH 7.0) using 10 kDa Centricon filters. The concentration of the Mb variants (ferric
15 form) was determined using the following extinction coefficients: $\epsilon_{410}=157 \text{ mM}^{-1}\text{cm}^{-1}$ for
16 Fe(ppIX)-containing variants and $\epsilon_{470}=60 \text{ mM}^{-1}\text{cm}^{-1}$ for Fe(DADP)-containing variants, which
17 was determined using the pyridine hemochrome assay.¹⁰⁰
18
19
20
21
22
23
24
25

26 **T_m determination.** Thermal denaturation experiments were carried out using a JASCO J-
27 1100 CD spectrophotometer equipped with variable temperature/wavelength denaturation analysis
28 software and samples of purified Mb variant at 3 μ M in 50 mM potassium phosphate buffer (pH
29 7.0). Thermal denaturation curves were measured by monitoring the change in molar ellipticity at
30 222 or 228 nm over a temperature range from 13°C to 100°C. The temperature increase was set to
31 0.5°C per minute with an equilibration time of 10 seconds. Data integration time for the melt curve
32 was set to 4 seconds with a bandwidth of 1 nm. Linear baselines for the folded (θ_f) and unfolded
33 state (θ_u) were generated using the low temperature ($\theta_f = m_f T + b_f$) and high temperature ($\theta_u = m_u$
34 $T + b_u$) equations fitted to the experimental data before and after global unfolding, respectively
35 Using these equations, the melt data were converted to fraction of folded protein (F_f) vs.
36 temperature plots and the resulting curve was fitted to a sigmoidal equation (θ_{fit}) via nonlinear
37 regression analysis in SigmaPlot from which apparent melting temperatures were derived. The
38 reported mean values and standard errors were derived from experiments performed at least in
39 duplicate.
40
41
42
43
44
45
46
47
48
49

50
51 **Reduction potential determination.** Reactions were carried out on a 1 mL scale in a
52 solution of KPi (50 mM, pH 7) containing xanthine (30 mM stock solution); protein; dye; catalase
53 (10 mg/mL stock solution); a mixture of glucose (1 M stock solution)/glucose oxidase (175 μ M
54 stock solution), and xanthine oxidase (175 μ M stock solution). In a sealed vial, a solution of buffer
55
56
57
58
59
60

1
2
3 containing glucose (5 mM final concentration), glucose oxidase (50 µg/mL final concentration),
4 and xanthine (300 µM final concentration) was degassed by bubbling argon for 3 min. A buffered
5 solution containing the myoglobin variant and dye was carefully degassed in a similar manner in
6 a sealed cuvette (the concentration of the dye was adjusted by titration to give an absorbance which
7 is approximately equal to that of the highest absorbance band in the protein spectra). The two
8 solutions were then mixed together via cannula, and then catalase (5 µg/mL final concentration)
9 and xanthine oxidase (50 nM final concentration) were added to initiate the two-electron oxidation
10 of xanthine to uric acid and the corresponding reduction of protein and dye. The reactions were
11 monitored by UV–Vis spectrophotometry and the data were plotted. The reduction potential was
12 determined by adding the standard reduction potential of dye to the value of the y intercept
13 obtained by fitting the data to the Nernst equation (Eq. 1).
14
15
16
17
18
19
20
21
22

$$E_{m.Dye} + \frac{RT}{nF} \ln \left(\frac{[Dye_{ox}]}{[Dye_{red}]} \right) = E_{m.Protein} + \frac{RT}{nF} \ln \left(\frac{[Protein_{ox}]}{[Protein_{red}]} \right) \quad (\text{Eq. 1})$$

23
24
25
26
27 The absorbance values corresponding to the protein (based on the Soret band of the oxidised form)
28 and the dye (Figure S3) were used to determine the ratio of concentrations of oxidized (ox) to
29 reduced (red) form of both protein and dye at each stage of the experiment (Eq. 2).
30
31
32

$$\frac{A - A_{\min}}{A_{\max} - A} = \frac{[\text{oxidised}]}{[\text{reduced}]} \quad (\text{Eq. 2})$$

33
34
35
36
37
38
39 **Cyclopropanation reactions.** General cyclopropanation reactions were carried out at a
40 400 µL-scale using 10 µM Mb variant, 10 mM styrene and 20 mM EDA. In a typical procedure,
41 potassium phosphate buffer (50 mM, pH 7.0) was degassed by bubbling argon into the mixture for
42 3 min in a sealed vial. A buffered solution containing the myoglobin variant was carefully degassed
43 in a similar manner in a separate vial. The two solutions were then mixed together via cannula.
44 Reactions were initiated by addition of 10 µL of styrene (from a 0.4 M stock solution in ethanol),
45 followed by the addition of 10 µL of EDA (from a 0.8 M stock solution in ethanol) with a syringe,
46 and the reaction mixture was stirred for 16 hours at room temperature, under positive argon
47 pressure. Aerobic reactions were carried out without degassing the solution with argon and in open
48 reaction vessels. Reactions with reductant were performed in a similar manner adding to the
49 potassium phosphate buffer 40 µL of sodium dithionite (100 mM stock solution in buffer).
50
51
52
53
54
55
56
57
58
59
60

1
2
3
4
5
6
7
8
9
10
11
12
13
14
15
16
17
18
19
20
21
22
23
24
25
26
27
28
29
30
31
32
33
34
35
36
37
38
39
40
41
42
43
44
45
46
47
48
49
50
51
52
53
54
55
56
57
58
59
60

Product analysis. The reactions were analyzed by adding 20 μL of internal standard (benzodioxole, 100 mM in methanol) to the reaction mixture, followed by extraction with 400 μL of dichloromethane (DCM) and analyzed by GC – FID (see the Analytical Methods in the Supporting Information). Calibration curves of the different cyclopropane products were constructed using synthetically produced authentic standards (see the Synthetic Procedures in the Supporting Information). All measurements were performed at least in duplicate. For each experiment, negative control samples containing either no enzyme or no reductant were included. For stereoselectivity determination, the samples were analyzed by chiral GC–FID or chiral SFC as described in the Supporting Information

Kinetic experiments. For the kinetic measurement, reactions were carried out on a 400 μL -scale in KPi buffer (pH 7.0) using 5 μM Mb variant, 2.5 mM vinyl benzoate (from a 0.2 M stock solution in ethanol) and 2.5 mM EDA (from a 0.2 M stock solution in ethanol). At regular intervals 20 μL of solution were collected and quenched with 50 μL of 0.2 M HCl. Aliquots were analysed by adding 20 μL of internal standard (benzodioxole, 50 mM in ethanol) followed by extraction with 400 μL of dichloromethane and analysis by gas chromatography (GC). For the Hammett analyses, reactions were carried out on a 400 μL scale in KPi buffer (pH 7.0) and 10% ethanol using 1 μM or 2 μM Mb variant (see Figure S6 and S7 for details), 1.25 mM substituted styrene (from a 0.1 M stock solution in ethanol), 1.25 mM styrene (from a 0.1 M stock solution in ethanol) and 2.5 mM EDA (from a 0.2 M stock solution in ethanol). The reactions were quenched after 2, 4 and 5 min by adding 100 μL of 0.2 M HCl and 20 μL of internal standard (benzodioxole, 50 mM in ethanol) to the reaction mixture. The products were extracted with 400 μL of dichloromethane and analysed by gas chromatography (GC). Representative kinetic plots corresponding to these experiments are reported in Figure S6 and S7.

Radical Spin Trap Experiments. Reactions were carried out on a 400 μL -scale using 10 μM Mb variant, 10 mM styrene, 20 mM EDA with or without 100 mM 4-hydroxy-2,2,6,6-tetramethylpiperidine 1-oxyl (TEMPO) or 5,5-Dimethyl-1-pyrroline N-oxide (DMPO), and 10 mM sodium dithionite. In a typical reaction, a solution containing sodium dithionite (100 mM stock solution) in potassium phosphate buffer (50 mM, pH 7.0, 10% dimethylformamide (DMF)) was degassed by bubbling argon into the mixture for 3 min in a septum-capped vial. A buffered solution containing the myoglobin variant was carefully degassed in a similar manner in a separate

1
2
3 vial. The two solutions were then mixed together via cannula. Reactions were initiated by addition
4 of 10 μL of styrene (from a 0.4 M stock solution in DMF), followed by the addition of radical trap
5 reagent (40 μL , 1M stock solution in DMF) and 10 μL of EDA (from a 0.8 M stock solution in
6 DMF) with a syringe. The reaction was stirred for 16 hours at room temperature, under positive
7 argon pressure. For product analysis, 20 μL of internal standard (benzodioxole, 50 mM in ethanol)
8 were added to the reaction mixture followed by extraction with 400 μL of dichloromethane and
9 analysis by gas chromatography (GC).
10
11
12
13
14
15

16 **Reactions with *cis*- β -deutero-styrene.** Reactions were carried out at 2 mL-scale using 60
17 μM Mb variant, 0.2 M *cis*- β - d_1 -styrene, 0.4 M ethyl diazoacetate (EDA). In a typical reaction,
18 potassium phosphate buffer (50 mM, pH 7.0, 10% DMF) was degassed by bubbling argon into the
19 mixture for 3 min in a sealed vial. A buffered solution containing the myoglobin variant was
20 carefully degassed in a similar manner in a separate vial. The two solutions were then mixed
21 together via cannula. Reactions were initiated by addition of *cis*- β - d_1 -styrene (42.1 mg, 0.40
22 mmol), followed by the addition of EDA (84.0 mL, 0.80 mmol) with a syringe. The reaction
23 mixture was stirred for 16 hours at room temperature, under positive argon pressure. The reaction
24 products were extracted with dichloromethane (2 mL, three times), and the organic layers were
25 collected and dried over MgSO_4 . The organic solvent was removed by rotary evaporation, and the
26 crude was purified via flash chromatography (silica gel, hexane:AcOEt 99:1). The analytical data
27 for 3a-d and 3b-d are in accord with those reported in literature. Enantiopure ***d*-5a_{cis}**: ^1H NMR (400
28 MHz, CDCl_3): δ 7.30 (t, $J = 7.2$ Hz, 2H), 7.22 (t, $J = 7.2$ Hz, 1H), 7.11 (d, $J = 7.2$ Hz, 2H), 4.20
29 (q, $J = 14.4$ Hz, 7.2 Hz, 2H), 2.53 (dd, $J = 9.2$ Hz, 4.0 Hz, 1H), 1.91 (t (=dd), $J = 4.0$ Hz, 1H), 1.61
30 (dd, $J = 8.9$ Hz, 5.2 Hz, 1H), 1.30 (t, $J = 7.2$ Hz, 3H) ppm. ^2H NMR (60 MHz, CDCl_3): δ 1.32 ppm
31 (s, 1H). Enantiopure ***d*-5a_{trans}**: ^1H NMR (400 MHz, CDCl_3): δ 7.28-7.21 (m, 2H), 7.16 (t, $J = 7.1$
32 Hz, 1H), 7.06 (d, $J = 7.2$ Hz, 2H), 3.83 (q, $J = 7.1$ Hz, 2H), 2.54 (t, $J = 9.0$ Hz, 1H), 2.03 (t, $J =$
33 8.5 Hz, 1H), 1.28 (d, $J = 7.0$ Hz, 1H), 0.93 ppm (t, $J = 7.1$ Hz, 3H). ^2H NMR (60 MHz, CDCl_3): δ
34 1.72 ppm (s, 1H).
35
36
37
38
39
40
41
42
43
44
45
46
47
48
49
50
51
52
53
54
55
56
57
58
59
60

ASSOCIATED CONTENT

Supporting Information

Supporting information includes supplementary Tables and Figures, synthetic procedures, analytical methods, and compound characterization data.

AUTHOR INFORMATION

Corresponding Authors

* rfasan@ur.rochester.edu.

ACKNOWLEDGMENT

This work was supported by the U.S. National Institute of Health grant GM098628. MS instrumentation was supported by the U.S. NSF grant CHE-0946653.

REFERENCES

- (1) Doyle, M. P., and Forbes, D. C. Recent Advances in Asymmetric Catalytic Metal Carbene Transformations, *Chem. Rev.* **1998**, *98*, 911-936.
- (2) Lebel, H., Marcoux, J. F., Molinaro, C., and Charette, A. B. Stereoselective cyclopropanation reactions, *Chem. Rev.* **2003**, *103*, 977-1050.
- (3) Davies, H. M. L., and Hedley, S. J. Intermolecular reactions of electron-rich heterocycles with copper and rhodium carbenoids, *Chem. Soc. Rev.* **2007**, *36*, 1109-1119.
- (4) Pellissier, H. Recent developments in asymmetric cyclopropanation, *Tetrahedron* **2008**, *64*, 7041-7095.
- (5) Davies, H. M. L., and Denton, J. R. Application of donor/acceptor-carbenoids to the synthesis of natural products, *Chem. Soc. Rev.* **2009**, *38*, 3061-3071.
- (6) Reichelt, A., and Martin, S. F. Synthesis and properties of cyclopropane-derived peptidomimetics, *Acc. Chem. Res.* **2006**, *39*, 433-442.
- (7) Talele, T. T. The "Cyclopropyl Fragment" is a Versatile Player that Frequently Appears in Preclinical/Clinical Drug Molecules, *J. Med. Chem.* **2016**, *59*, 8712-8756.
- (8) Ebner, C., and Carreira, E. M. Cyclopropanation Strategies in Recent Total Syntheses, *Chem. Rev.* **2017**, *117*, 11651-11679.
- (9) Bordeaux, M., Tyagi, V., and Fasan, R. Highly Diastereoselective and Enantioselective Olefin Cyclopropanation Using Engineered Myoglobin-Based Catalysts, *Angew. Chem. Int. Ed.* **2015**, *54*, 1744-1748.

- 1
2
3 (10) Bajaj, P., Sreenilayam, G., Tyagi, V., and Fasan, R. Gram-Scale Synthesis of Chiral
4 Cyclopropane-Containing Drugs and Drug Precursors with Engineered Myoglobin
5 Catalysts Featuring Complementary Stereoselectivity, *Angew. Chem. Int. Ed.* **2016**, *55*,
6 16110–16114.
7
8 (11) Tinoco, A., Steck, V., Tyagi, V., and Fasan, R. Highly Diastereo- and Enantioselective
9 Synthesis of Trifluoromethyl-Substituted Cyclopropanes via Myoglobin-Catalyzed
10 Transfer of Trifluoromethylcarbene, *J. Am. Chem. Soc.* **2017**, *139*, 5293-5296.
11 (12) Chandgude, A. L., and Fasan, R. Highly Diastereo- and Enantioselective Synthesis of
12 Nitrile-Substituted Cyclopropanes by Myoglobin-Mediated Carbene Transfer Catalysis,
13 *Angew. Chem. Int. Ed.* **2018**, *57*, 15852-15856.
14 (13) Vargas, D., Khade, R., Zhang, Y., and Fasan, R. Biocatalytic strategy for highly diastereo-
15 and enantioselective synthesis of 2,3-dihydrobenzofuran based tricyclic scaffolds., *Angew.*
16 *Chem. Int. Ed.* **2019**, *58*, 10148-10152.
17 (14) Coelho, P. S., Brustad, E. M., Kannan, A., and Arnold, F. H. Olefin Cyclopropanation via
18 Carbene Transfer Catalyzed by Engineered Cytochrome P450 Enzymes, *Science* **2013**,
19 *339*, 307-310.
20 (15) Gober, J. G., Rydeen, A. E., Gibson-O'Grady, E. J., Leuthaeuser, J. B., Fetrow, J. S., and
21 Brustad, E. M. Mutating a Highly Conserved Residue in Diverse Cytochrome P450s
22 Facilitates Diastereoselective Olefin Cyclopropanation, *Chembiochem* **2016**, *17*, 394-397.
23 (16) Knight, A. M., Kan, S. B. J., Lewis, R. D., Brandenburg, O. F., Chen, K., and Arnold, F.
24 H. Diverse Engineered Heme Proteins Enable Stereodivergent Cyclopropanation of
25 Unactivated Alkenes, *ACS Central Sci.* **2018**, *4*, 372-377.
26 (17) Brandenburg, O. F., Prier, C. K., Chen, K., Knight, A. M., Wu, Z., and Arnold, F. H.
27 Stereoselective Enzymatic Synthesis of Heteroatom-Substituted Cyclopropanes, *ACS*
28 *Catal.* **2018**, *8*, 2629-2634.
29 (18) Chen, K., Zhang, S. Q., Brandenburg, O. F., Hong, X., and Arnold, F. H. Alternate Heme
30 Ligation Steers Activity and Selectivity in Engineered Cytochrome P450-Catalyzed
31 Carbene-Transfer Reactions, *J. Am. Chem. Soc.* **2018**, *140*, 16402-16407.
32 (19) Srivastava, P., Yang, H., Ellis-Guardiola, K., and Lewis, J. C. Engineering a dirhodium
33 artificial metalloenzyme for selective olefin cyclopropanation, *Nat. Commun.* **2015**, *6*,
34 7789.
35 (20) Sreenilayam, G., Moore, E. J., Steck, V., and Fasan, R. Metal substitution modulates the
36 reactivity and extends the reaction scope of myoglobin carbene transfer catalysts, *Adv.*
37 *Synth. Cat.* **2017**, *359*, 2076–2089.
38 (21) Sreenilayam, G., Moore, E. J., Steck, V., and Fasan, R. Stereoselective olefin
39 cyclopropanation under aerobic conditions with an artificial enzyme incorporating an iron-
40 chlorin e6 cofactor, *ACS Catal.* **2017**, *7*, 7629-7633.
41 (22) Dydio, P., Key, H. M., Nazarenko, A., Rha, J. Y. E., Seyedkazemi, V., Clark, D. S., and
42 Hartwig, J. F. An artificial metalloenzyme with the kinetics of native enzymes, *Science*
43 **2016**, *354*, 102-106.
44 (23) Wolf, M. W., Vargas, D. A., and Lehnert, N. Engineering of RuMb: Toward a Green
45 Catalyst for Carbene Insertion Reactions, *Inorg. Chem.* **2017**, *56*, 5623-5635.
46 (24) Ohora, K., Meichin, H., Zhao, L. M., Wolf, M. W., Nakayama, A., Hasegawa, J., Lehnert,
47 N., and Hayashi, T. Catalytic Cyclopropanation by Myoglobin Reconstituted with Iron
48 Porphycene: Acceleration of Catalysis due to Rapid Formation of the Carbene Species, *J.*
49 *Am. Chem. Soc.* **2017**, *139*, 17265-17268.
50
51
52
53
54
55
56
57
58
59
60

- 1
2
3 (25) Villarino, L., Splan, K. E., Reddem, E., Alonso-Cotchico, L., de Souza, C. G., Lledos, A.,
4 Marechal, J. D., Thunnissen, A. M. W. H., and Roelfes, G. An Artificial Heme Enzyme for
5 Cyclopropanation Reactions, *Angew. Chem. Int. Ed.* **2018**, *57*, 7785-7789.
- 6 (26) Khade, R. L., and Zhang, Y. Catalytic and Biocatalytic Iron Porphyrin Carbene Formation:
7 Effects of Binding Mode, Carbene Substituent, Porphyrin Substituent, and Protein Axial
8 Ligand, *J. Am. Chem. Soc.* **2015**, *137*, 7560-7563.
- 9 (27) Wei, Y., Tinoco, A., Steck, V., Fasan, R., and Zhang, Y. Cyclopropanations via Heme
10 Carbenes: Basic Mechanism and Effects of Carbene Substituent, Protein Axial Ligand, and
11 Porphyrin Substitution, *J. Am. Chem. Soc.* **2018**, *140*, 1649-1662.
- 12 (28) Lewis, R. D., Garcia-Borras, M., Chalkley, M. J., Buller, A. R., Houk, K. N., Kan, S. B. J.,
13 and Arnold, F. H. Catalytic iron-carbene intermediate revealed in a cytochrome c carbene
14 transferase, *Proc. Natl. Acad. Sci. USA* **2018**, *115*, 7308-7313.
- 15 (29) Tinoco, A., Wei, Y., Bacik, J.-P., Carminati, D. M., Moore, E. J., Ando, N., Zhang, Y., and
16 Fasan, R. Origin of High Stereocontrol in Olefin Cyclopropanation Catalyzed by an
17 Engineered Carbene Transferase, *ACS Catal.* **2019**, *9* 1514-1524
- 18 (30) Tyagi, V., Sreenilayam, G., Bajaj, P., Tinoco, A., and Fasan, R. Biocatalytic Synthesis of
19 Allylic and Allenyl Sulfides through a Myoglobin-Catalyzed Doyle-Kirmse Reaction,
20 *Angew. Chem. Int. Ed.* **2016**, *55*, 13562-13566.
- 21 (31) Tyagi, V., and Fasan, R. Myoglobin-Catalyzed Olefination of Aldehydes, *Angew. Chem.*
22 *Int. Ed.* **2016**, *55*, 2512-2516
- 23 (32) Vargas, D. A., Tinoco, A., Tyagi, V., and Fasan, R. Myoglobin-Catalyzed C-H
24 Functionalization of Unprotected Indoles, *Angew. Chem. Int. Ed.* **2018**, *57*, 9911-9915.
- 25 (33) Gnad, F., and Reiser, O. Synthesis and applications of beta-aminocarboxylic acids
26 containing a cyclopropane ring, *Chemical Reviews* **2003**, *103*, 1603-1623.
- 27 (34) Wong, H. N. C., Hon, M. Y., Tse, C. W., Yip, Y. C., Tanko, J., and Hudlicky, T. Use of
28 Cyclopropanes and Their Derivatives in Organic-Synthesis, *Chem. Rev.* **1989**, *89*, 165-198.
- 29 (35) Danishefsky, S. Electrophilic Cyclopropanes in Organic-Synthesis, *Acc. Chem. Res.* **1979**,
30 *12*, 66-72.
- 31 (36) Marshall, N. M., Garner, D. K., Wilson, T. D., Gao, Y. G., Robinson, H., Nilges, M. J.,
32 and Lu, Y. Rationally tuning the reduction potential of a single cupredoxin beyond the
33 natural range, *Nature* **2009**, *462*, 113-U127.
- 34 (37) Bhagi-Damodaran, A., Petrik, I. D., Marshall, N. M., Robinson, H., and Lu, Y. Systematic
35 Tuning of Heme Redox Potentials and Its Effects on O₂ Reduction Rates in a Designed
36 Oxidase in Myoglobin, *J. Am. Chem. Soc.* **2014**, *136*, 11882-11885.
- 37 (38) Mirts, E. N., Bhagi-Damodaran, A., and Lu, Y. Understanding and Modulating
38 Metalloenzymes with Unnatural Amino Acids, Non-Native Metal Ions, and Non-Native
39 Metallocofactors, *Acc. Chem. Res.* **2019**, *52*, 935-944.
- 40 (39) Oohora, K., Kihira, Y., Mizohata, E., Inoue, T., and Hayashi, T. C(sp³)-H Bond
41 Hydroxylation Catalyzed by Myoglobin Reconstituted with Manganese Porphycene, *J.*
42 *Am. Chem. Soc.* **2013**, *135*, 17282-17285.
- 43 (40) Oohora, K., Onoda, A., and Hayashi, T. Hemoproteins Reconstituted with Artificial Metal
44 Complexes as Biohybrid Catalysts, *Acc. Chem. Res.* **2019**, *52*, 945-954.
- 45 (41) Onderko, E. L., Silakov, A., Yosca, T. H., and Green, M. T. Characterization of a
46 selenocysteine-ligated P450 compound I reveals direct link between electron donation and
47 reactivity, *Nat. Chem.* **2017**, *9*, 623-628.
- 48
49
50
51
52
53
54
55
56
57
58
59
60

- 1
2
3 (42) Moore, E. J., and Fasan, R. Effect of proximal ligand substitutions on the carbene and
4 nitrene transferase activity of myoglobin, *Tetrahedron* **2019**, *75*, 2357-2363.
- 5 (43) Coelho, P. S., Wang, Z. J., Ener, M. E., Baril, S. A., Kannan, A., Arnold, F. H., and Brustad,
6 E. M. A serine-substituted P450 catalyzes highly efficient carbene transfer to olefins in
7 vivo, *Nat. Chem. Biol.* **2013**, *9*, 485-487.
- 8 (44) Hyster, T. K., Farwell, C. C., Buller, A. R., McIntosh, J. A., and Arnold, F. H. Enzyme-
9 Controlled Nitrogen-Atom Transfer Enables Regiodivergent C-H Amination, *J. Am. Chem.*
10 *Soc.* **2014**, *136*, 15505-15508.
- 11 (45) Green, A. P., Hayashi, T., Mittl, P. R. E., and Hilyert, D. A Chemically Programmed
12 Proximal Ligand Enhances the Catalytic Properties of a Heme Enzyme, *J. Am. Chem. Soc.*
13 **2016**, *138*, 11344-11352.
- 14 (46) Pott, M., Hayashi, T., Mori, T., Mittl, P. R. E., Green, A. P., and Hilvert, D. A
15 Noncanonical Proximal Heme Ligand Affords an Efficient Peroxidase in a Globin Fold, *J.*
16 *Am. Chem. Soc.* **2018**, *140*, 1535-1543.
- 17 (47) Hayashi, T., Tinzl, M., Mori, T., Krenzel, U., Proppe, J., Soetbeer, J., Klose, D., Jeschke,
18 G., Reiher, M., and Hilvert, D. Capture and characterization of a reactive haem-carbenoid
19 complex in an artificial metalloenzyme, *Nat. Catal.* **2018**, *1*, 578-584.
- 20 (48) Neya, S., Nagai, M., Nagatomo, S., Hoshino, T., Yoneda, T., and Kawaguchi, A. T. Utility
21 of heme analogues to intentionally modify heme-globin interactions in myoglobin,
22 *Biochimica Et Biophysica Acta-Bioenergetics* **2016**, *1857*, 582-588.
- 23 (49) Bordeaux, M., Singh, R., and Fasan, R. Intramolecular C(sp³)H amination of arylsulfonyl
24 azides with engineered and artificial myoglobin-based catalysts, *Bioorg. Med. Chem.* **2014**,
25 *22*, 5697-5704.
- 26 (50) Moore, E. J., Steck, V., Bajaj, P., and Fasan, R. Chemoselective Cyclopropanation over
27 Carbene Y-H Insertion Catalyzed by an Engineered Carbene Transferase, *J. Org. Chem.*
28 **2018**, *83*, 7480-7490.
- 29 (51) Springer, B. A., Sligar, S. G., Olson, J. S., and Phillips, G. N. Mechanisms of Ligand
30 Recognition in Myoglobin, *Chem. Rev.* **1994**, *94*, 699-714.
- 31 (52) Chen, Y., Ruppel, J. V., and Zhang, X. P. Cobalt-catalyzed asymmetric cyclopropanation
32 of electron-deficient olefins, *J. Am. Chem. Soc.* **2007**, *129*, 12074-+.
- 33 (53) Wang, H. B., Guptill, D. M., Varela-Alvarez, A., Musaev, D. G., and Davies, H. M. L.
34 Rhodium-catalyzed enantioselective cyclopropanation of electron-deficient alkenes,
35 *Chem. Sci.* **2013**, *4*, 2844-2850.
- 36 (54) Lindsay, V. N. G., Fiset, D., Gritsch, P. J., Azzi, S., and Charette, A. B. Stereoselective
37 Rh-2(S-IBAZ)(4)-Catalyzed Cyclopropanation of Alkenes, Alkynes, and Allenes:
38 Asymmetric Synthesis of Diacceptor Cyclopropylphosphonates and
39 Alkylidenecyclopropanes, *J. Am. Chem. Soc.* **2013**, *135*, 1463-1470.
- 40 (55) Shiro, Y., Iizuka, T., Marubayashi, K., Ogura, T., Kitagawa, T., Balasubramanian, S., and
41 Boxer, S. G. Spectroscopic Study of Ser92 Mutants of Human Myoglobin - Hydrogen-
42 Bonding Effect of Ser92 to Proximal His93 on Structure and Property of Myoglobin,
43 *Biochemistry* **1994**, *33*, 14986-14992.
- 44 (56) Decatur, S. M., Belcher, K. L., Rickert, P. K., Franzen, S., and Boxer, S. G. Hydrogen
45 bonding modulates binding of exogenous ligands in a myoglobin proximal cavity mutant,
46 *Biochemistry* **1999**, *38*, 11086-11092.
- 47
48
49
50
51
52
53
54
55
56
57
58
59
60

- 1
2
3 (57) Kawakami, N., Shoji, O., and Watanabe, Y. Single-Step Reconstitution of Apo-
4 Hemoproteins at the Disruption Stage of Escherichia coli Cells, *Chembiochem* **2012**, *13*,
5 2045-2047.
6
7 (58) Wang, L., and Schultz, P. G. Expanding the genetic code, *Angew. Chem. Int. Ed.* **2004**, *44*,
8 34-66.
9 (59) Xiao, H., Peters, F. B., Yang, P. Y., Reed, S., Chittuluru, J. R., and Schultz, P. G. Genetic
10 Incorporation of Histidine Derivatives Using an Engineered Pyrrolysyl-tRNA Synthetase,
11 *ACS Chem. Biol.* **2014**, *9*, 1092-1096.
12 (60) Moore, E. J., Zorine, D., Hansen, W. A., Khare, S. D., and Fasan, R. Enzyme stabilization
13 via computationally guided protein stapling, *Proc. Natl. Acad. Sci. USA* **2017**, *114*, 12472-
14 12477.
15 (61) Efimov, I., Parkin, G., Millett, E. S., Glenday, J., Chan, C. K., Weedon, H., Randhawa, H.,
16 Basran, J., and Raven, E. L. A simple method for the determination of reduction potentials
17 in heme proteins, *FEBS Lett.* **2014**, *588*, 701-704.
18 (62) Battistuzzi, G., Bellei, M., Casella, L., Bortolotti, C. A., Roncone, R., Monzani, E., and
19 Sola, M. Redox reactivity of the heme Fe³⁺/Fe²⁺ couple in native myoglobins and mutants
20 with peroxidase-like activity, *J. Biol. Inorg. Chem.* **2007**, *12*, 951-958.
21 (63) Bickar, D., Bonaventura, C., and Bonaventura, J. Carbon-Monoxide Driven Reduction of
22 Ferric Heme and Heme-Proteins, *J. Biol. Chem.* **1984**, *259*, 777-783.
23 (64) Salomon, R. G., and Kochi, J. K. Copper(I) Catalysis in Cyclopropanations with Diazo-
24 Compounds - Role of Olefin Coordination, *J. Am. Chem. Soc.* **1973**, *95*, 3300-3310.
25 (65) Wolf, J. R., Hamaker, C. G., Djukic, J. P., Kodadek, T., and Woo, L. K. Shape and
26 Stereoselective Cyclopropanation of Alkenes Catalyzed by Iron Porphyrins, *J. Am. Chem.*
27 *Soc.* **1995**, *117*, 9194-9199.
28 (66) Lai, T. S., Chan, F. Y., So, P. K., Ma, D. L., Wong, K. Y., and Che, C. M. Alkene
29 cyclopropanation catalyzed by Halterman iron porphyrin: participation of organic bases as
30 axial ligands, *Dalton T.* **2006**, 4845-4851.
31 (67) Simkhovich, L., Mahammed, A., Goldberg, I., and Gross, Z. Synthesis and characterization
32 of germanium, tin, phosphorus, iron, and rhodium complexes of
33 tris(pentafluorophenyl)corrole, and the utilization of the iron and rhodium corroles as
34 cyclopropanation catalysts, *Chem. Eur. J.* **2001**, *7*, 1041-1055.
35 (68) Renata, H., Wang, Z. J., Kitto, R. Z., and Arnold, F. H. P450-catalyzed asymmetric
36 cyclopropanation of electron-deficient olefins under aerobic conditions, *Catal. Sci.*
37 *Technol.* **2014**, *4*, 3640-3643.
38 (69) Chapman, N. B., and Shorter, J. (1982) *Correlation analysis of organic reactivity*, Plenum
39 Press, New York.
40 (70) Singh, R., Kolev, J. N., Sutera, P. A., and Fasan, R. Enzymatic C(sp³)-H Amination:
41 P450-Catalyzed Conversion of Carbonazidates into Oxazolidinones, *ACS Catal.* **2015**, *5*,
42 1685-1691.
43 (71) Ji, G. Z., Jiang, X. K., Zhang, Y. H., Yuan, S. G., Yu, C. X., Shi, Y. Q., Zhang, X. L., and
44 Shi, W. T. The Spin Delocalization Substituent Parameter Sigma-Jj .5. Correlation-
45 Analysis of F-19 Chemical-Shifts of Substituted Trifluorostyrenes - the Unresolved Polar
46 Substituent Parameter Sigma-Mb, *J. Phys. Org. Chem.* **1990**, *3*, 643-650.
47 (72) Jiang, X. K., and Ji, G. Z. A Self-Consistent and Cross-Checked Scale of Spin-
48 Delocalization Substituent Constants, the Sigma.(Jj) Scale, *J. Org. Chem.* **1992**, *57*, 6051-
49 6056.
50
51
52
53
54
55
56
57
58
59
60

- 1
2
3 (73) Dincturk, S., and Jackson, R. A. Free-Radical Reactions in Solution .7. Substituent Effects
4 on Free-Radical Reactions - Comparison of the Sigma-Scale with Other Measures of
5 Radical Stabilization, *J. Chem. Soc. Perk. T.* **1981**, 1127-1131.
- 6 (74) Kim, S. S., Zhu, Y., and Lee, K. H. Thermal isomerizations of ketenimines to nitriles:
7 Evaluations of sigma-dot (sigma(center dot)) constants for spin-delocalizations, *J. Org.*
8 *Chem.* **2000**, *65*, 2919-2923.
- 9 (75) Jiang, X. K. Establishment and successful application of the sigma(JJ)center dot scale of
10 spin-delocalization substituent constants, *Acc. Chem. Res.* **1997**, *30*, 283-289.
- 11 (76) Dzik, W. I., Xu, X., Zhang, X. P., Reek, J. N. H., and de Bruin, B. 'Carbene Radicals' in
12 CoII(por)-Catalyzed Olefin Cyclopropanation, *J. Am. Chem. Soc.* **2010**, *132*, 10891-10902.
- 13 (77) Lu, H., Dzik, W. I., Xu, X., Wojtas, L., de Bruin, B., and Zhang, X. P. Experimental
14 Evidence for Cobalt(III)-Carbene Radicals: Key Intermediates in Cobalt(II)-Based
15 Metalloradical Cyclopropanation, *J. Am. Chem. Soc.* **2011**, *133*, 8518-8521.
- 16 (78) Edulji, S. K., and Nguyen, S. T. Catalytic olefin cyclopropanation using mu-oxo-
17 bis[(salen)iron(III)] complexes, *Organometallics* **2003**, *22*, 3374-3381.
- 18 (79) Intrieri, D., Le Gac, S., Caselli, A., Rose, E., Boitrel, B., and Gallo, E. Highly
19 diastereoselective cyclopropanation of alpha-methylstyrene catalysed by a C-2-
20 symmetrical chiral iron porphyrin complex, *Chem. Commun.* **2014**, *50*, 1811-1813.
- 21 (80) Carminati, D. M., Intrieri, D., Caselli, A., Le Gac, S., Boitrel, B., Toma, L., Legnani, L.,
22 and Gallo, E. Designing 'Totem' C2 -Symmetrical Iron Porphyrin Catalysts for
23 Stereoselective Cyclopropanations, *Chemistry* **2016**, *22*, 13599-135612.
- 24 (81) Morandi, B., and Carreira, E. M. Iron-Catalyzed Cyclopropanation in 6 M KOH with in
25 Situ Generation of Diazomethane, *Science* **2012**, *335*, 1471-1474.
- 26 (82) Liu, J., Hu, L., Wang, L., Chen, H., and Deng, L. An Iron(II) Ylide Complex as a Masked
27 Open-Shell Iron Alkylidene Species in Its Alkylidene-Transfer Reactions with Alkenes, *J.*
28 *Am. Chem. Soc.* **2017**, *139*, 3876-3888.
- 29 (83) Li, Y., Huang, J. S., Zhou, Z. Y., Che, C. M., and You, X. Z. Remarkably stable iron
30 porphyrins bearing nonheteroatom-stabilized carbene or (Alkoxy carbonyl) carbenes:
31 Isolation, X-ray crystal structures, and carbon atom transfer reactions with hydrocarbons,
32 *J. Am. Chem. Soc.* **2002**, *124*, 13185-13193.
- 33 (84) Che, C. M., Huang, J. S., Lee, F. W., Li, Y., Lai, T. S., Kwong, H. L., Teng, P. F., Lee, W.
34 S., Lo, W. C., Peng, S. M., and Zhou, Z. Y. Asymmetric inter- and intramolecular
35 cyclopropanation of alkenes catalyzed by chiral ruthenium porphyrins. Synthesis and
36 crystal structure of a chiral metalloporphyrin carbene complex, *J. Am. Chem. Soc.* **2001**,
37 *123*, 4119-4129.
- 38 (85) Anding, B. J., Ellern, A., and Woo, L. K. Olefin Cyclopropanation Catalyzed by
39 Iridium(III) Porphyrin Complexes, *Organometallics* **2012**, *31*, 3628-3635.
- 40 (86) Kwong, H. L., Wong, W. L., Lee, W. S., Cheng, L. S., and Wong, W. T. New chiral 2,2':
41 6',2"-terpyridine ligands from the chiral pool: synthesis, crystal structure of a rhodium
42 complex and uses in copper- and rhodium-catalyzed enantioselective cyclopropanation of
43 styrene, *Tetrahedron-Asymmetr.* **2001**, *12*, 2683-2694.
- 44 (87) Diaz-Requejo, M. M., Perez, P. J., Brookhart, M., and Templeton, J. L. Substituent effects
45 on the reaction rates of copper-catalyzed cyclopropanation and aziridination of para-
46 substituted styrenes, *Organometallics* **1997**, *16*, 4399-4402.
- 47 (88) Kwong, H. L., Cheng, L. S., Lee, W. S., Wong, W. L., and Wong, W. T. Novel chiral di-
48 2-pyridyl ketone ligands: Crystal structure of a copper complex and its activity in the
49
50
51
52
53
54
55
56
57
58
59
60

- copper-catalyzed enantioselective cyclopropanation of styrene, *Eur. J. Inorg. Chem.* **2000**, 1997-2002.
- (89) Mahandru, G. M., Liu, G., and Montgomery, J. Ligand-dependent scope and divergent mechanistic behavior in nickel-catalyzed reductive couplings of aldehydes and alkynes, *J. Am. Chem. Soc.* **2004**, *126*, 3698-3699.
- (90) Lee, Y. C., Patil, S., Golz, C., Strohmam, C., Ziegler, S., Kumar, K., and Waldmann, H. A ligand-directed divergent catalytic approach to establish structural and functional scaffold diversity, *Nat. Commun.* **2017**, *8*.
- (91) Chandgude, A. L., Ren, X., and Fasan, R. Stereodivergent Intramolecular Cyclopropanation Enabled by Engineered Carbene Transferases, *J. Am. Chem. Soc.* **2019**, *141*, 9145-9150.
- (92) Shaik, S., Hirao, H., and Kumar, D. Reactivity of high-valent iron-oxo species in enzymes and synthetic reagents: A tale of many states, *Acc. Chem. Res.* **2007**, *40*, 532-542.
- (93) Meunier, B., de Visser, S. P., and Shaik, S. Mechanism of oxidation reactions catalyzed by cytochrome P450 enzymes, *Chem. Rev.* **2004**, *104*, 3947-3980.
- (94) Tinoco, A., Wei, Y., Bacik, J.-P., Carminati, D. M., Moore, E. J., Ando, N., Zhang, Y., and Fasan, R. Origin of High Stereocontrol in Olefin Cyclopropanation Catalyzed by an Engineered Carbene Transferase, *ACS Catalysis* **2019**, *9*, 1514-1524.
- (95) Wei, Y., Tinoco, A., Steck, V., Fasan, R., and Zhang, Y. Cyclopropanations via Heme Carbenes: Basic Mechanism and Effects of Carbene Substituent, Protein Axial Ligand, and Porphyrin Substitution, *J. Am. Chem. Soc.* **2018**, *140*, 1649-1662.
- (96) Prier, C. K., Rankic, D. A., and MacMillan, D. W. C. Visible Light Photoredox Catalysis with Transition Metal Complexes: Applications in Organic Synthesis, *Chem. Rev.* **2013**, *113*, 5322-5363.
- (97) Lu, H. J., and Zhang, X. P. Catalytic C-H functionalization by metalloporphyrins: recent developments and future directions, *Chem. Soc. Rev.* **2011**, *40*, 1899-1909.
- (98) Studer, A., and Curran, D. P. Catalysis of Radical Reactions: A Radical Chemistry Perspective, *Angew. Chem. Int. Ed.* **2016**, *55*, 58-102.
- (99) Kuijpers, P. F., van der Vlugt, J. I., Schneider, S., and de Bruin, B. Nitrene Radical Intermediates in Catalytic Synthesis, *Chem. Eur. J.* **2017**, *23*, 13819-13829.
- (100) Berry, E. A., and Trumppower, B. L. Simultaneous Determination of Hemes-a, Hemes-B, and Hemes-C from Pyridine Hemochrome Spectra, *Analyt. Biochem.* **1987**, *161*, 1-15.

Graphical Abstract

